

MECHANICS AND DYNAMICS OF CIRCULAR MILLING OPERATION

by

NIMET KARDES

B.Sc., Istanbul Technical University, Istanbul, Turkey, 2002

A THESIS SUBMITTED IN PARTIAL FULFILLMENT OF
THE REQUIREMENTS FOR THE DEGREE OF
MASTER OF APPLIED SCIENCE

in

THE FACULTY OF GRADUATE STUDIES
(Mechanical Engineering)

THE UNIVERSITY OF BRITISH COLUMBIA

March 2005

© Nimet Kardes, 2005

Abstract

This thesis presents modeling of the mechanics and dynamics of circular milling operations.

With the recent advances in CNC machine tools which have high contouring accuracy, the circular milling operations are used in high speed opening of pockets in die, mold and aerospace machining industry. While the cutter rotates around the spindle axis, it follows a circular-trochoidal path, avoiding momentary pauses to change feed directions. The cutter engagement conditions, hence the chip thickness, the cutting force directions and amplitudes, and the dynamic stability of the milling process continuously change in circular milling operations. This thesis presents the first research in modeling the mechanics and dynamics of circular milling operations in the literature.

The kinematics of the chip removal generation is first modeled by considering the rigid body motions of the cutter and cutting edges. The time varying chip load and the resulting milling forces are predicted with experimental validation.

The dynamic stability of the process is complicated by three factors. The system dynamics has two delay terms and two periodic behaviours. Additionally the parameters of the coupled differential equations have time varying coefficients. First, the stability of the system is solved by taking the averages of the periodic coefficients in the frequency domain. The stability law developed by Altintas and Budak are extended to the circular milling.

Two alternative methods were studied to improve the frequency domain stability solution. The direct method proposed by Olgac and Sipahi, converged to the frequency domain solution since the assumptions were identical. The Time Finite Element method proposed by Stepan, Bayly and Mann is a numerical, time domain method where the time varying directional coefficients can be considered. To simplify the time finite element solution and decrease the computation time, only the most flexible mode in each direction was taken into account. The experiments were conducted to verify the proposed dynamic models and the simulation results obtained from frequency domain solution and time finite element method were compared against experimental

results. Both methods gave reasonable results only for speed independent and low axial depth of cut region but they are not able to predict the stability of a circular milling operation accurately.

Table of Contents

Abstract	ii
Table of Contents	iv
List of Tables	vi
List of Figures	vii
Acknowledgement	ix
Nomenclature	x
1.Introduction	1
2.Literature Review	3
2.1.Introduction	3
2.2.Mechanics of Milling Operation	3
2.3.Dynamics of Milling Operation	7
2.3.1.Tlusty's Approximate Solution	10
2.3.2.Opitz's Approximate Solution	12
2.3.3.Altintas & Budak's Frequency Domain Solution	15
2.3.4.Bayly's Time Domain Solution	16
2.3.5.Solution of a Linear Time Invariant Systems with a Time Delay	17
3.Mechanics of Circular Milling	19
3.1.Introduction	19
3.2.Geometric Modeling of Tool and Workpiece Intersection	21

3.2.1.Entry Transient Zone	22
3.2.2.Steady State Zone	25
3.2.3.Exit Transient Zone	26
3.3.Cutting Force Formulation	26
3.4.Simulations and Experimental Results	30
4.Direct Method for Chatter Stability of Milling Operation	34
4.1.Introduction	34
4.2.Direct Method	35
4.3.Stability of a Single Degree of Freedom Milling Operation	42
4.4.Simulations	48
5. Dynamics of Circular Milling Operation	52
5.1.Introduction	52
5.2.Dynamics of Circular Milling	52
5.3.Analytical Chatter Stability	55
5.3.1.Frequency Domain Solution	55
5.3.2.Time Finite Element Analysis (TFEA)	61
5.4.Simulations and Experimental Results	70
6.Conclusion	77
6.1.Conclusion	77
6.2.Future Research Directions	79
Bibliography	80

List of Tables

Table 5.1 :Modal parameters in x direction	71
Table 5.2 :Modal parameters in y direction	71
Table 5.3 :Axial depth of cut and spindle speed values for cutting tests and simulations	72
Table 5.4 :Common cutting conditions	72

List of Figures

Figure 2.1 :Milling operation	3
Figure 2.2 :Face, up and down milling	5
Figure 2.3 :Orthogonal and oblique cutting operations	6
Figure 2.4 :Dynamic chip generation in milling	8
Figure 2.5 :Regeneration mechanism in orthogonal cutting	8
Figure 2.6 :Tlusty's stability model for half immersion up milling	12
Figure 2.7 :Single degree of freedom interrupted turning model	16
Figure 3.1 :Formation of a slot by using circular milling (Source: Sandvik Coromant)	19
Figure 3.2 :Top view of circular milling	20
Figure 3.3 :Tool positions during operation	27
Figure 3.4 :Cutting forces in tangential and radial direction	29
Figure 3.5 :Simulated cutting forces in x and y directions	31
Figure 3.6 :Measured cutting forces in x and y directions	31
Figure 3.7 :Comparison of measured and simulated cutting forces at a small time window	32
Figure 3.8 :Variation of exit angle during the rotation of the tool around the workpiece	32
Figure 3.9 :Variation of chip thickness during the rotation of the tool around the workpiece	33
Figure 4.1 :Regenerative effect in milling operation	35
Figure 4.2 :A single degree of freedom milling system	43
Figure 4.3 :Comparison of direct method with frequency domain solution	49
Figure 4.4 :Comparison of direct method with experiments	50
Figure 5.1 :General representation of 2-DOF milling system	62
Figure 5.2 :Time finite element method developed for interrupted cutting operations	63
Figure 5.3 :Simulated displacements for a stable circular milling operation cutting conditions ($n=1500$ [rpm] and $b=6$ [mm], See Table 5.3)	73

Figure 5.4 :Simulated displacements for a stable circular milling operation cutting conditions

($n=7200$ [rpm] and $b=11$ [mm], See Table 5.3)

74

Figure 5.5 :Comparison of experimental and theoretical results

75

Acknowledgement

I would like to express my sincere gratitude and appreciation to my research supervisor Dr. Yusuf Altintas for the valuable instruction, guidance, support and encouragement which he has provided throughout my research at University of British Columbia. I would like to thank Nesrin Altintas for her hospitality.

I wish to thank my colleagues in the Manufacturing Automation Laboratory for sharing with me their knowledge and experience especially Doruk, Fuat and Kaan. I have a lot of good memories that I will remember forever. I feel very lucky to share the life with my close friends, Evren, Bahar, Gokhan, Kivilcim and my boyfriend, Ilter, during my stay in Canada. They were with me especially during tough times and made my life easier and enjoyable. I would also like to thank my friends in Turkey for their continuous presence and support.

Finally, I am deeply grateful to my beloved family, my mother Zuhale, my father Erol and my sister Demet for their lifelong love, encouragement, unwavering support and patience they have provided me throughout my entire life. This thesis and my all previous success are dedicated to them.

Nomenclature

a_x	directional milling coefficient in x direction
α_{x0}	average directional milling coefficient in x direction
\hat{a}_{qi}	coefficients of trial functions
$[A], [B], [G]$	constant state matrices
b	axial depth of cut
b_{lim}	critical axial depth of cut
c	step over feed
c_x	modal damping in x direction
d_{xx}	directional milling coefficient
$[D]$	directional milling coefficients matrix
$[D_0]$	average directional milling coefficients matrix
f	feed
F	resultant cutting force
F_r	radial cutting force
F_t	tangential cutting force
F_x	cutting force in the x direction
F_y	cutting force in the y direction
h	chip thickness
h_{int}	intended chip thickness

h_m	mean dynamic chip thickness
$[I]$	identity matrix
j	flute number
k	number of stability lobes
k_x	modal stiffness in x direction
K_c	cutting force coefficient
K_e	edge force coefficient
K_{fc}	feed cutting force coefficient
K_{fe}	feed edge force coefficient
K_{rc}	radial cutting force coefficient
K_{re}	radial edge force coefficient
K_r	ratio of radial to tangential force coefficient
K_{tc}	tangential cutting force coefficient
K_{te}	tangential edge force coefficient
K_s	resultant force coefficient
m_e	average number of teeth in cut
m_x	modal mass in x direction
n	spindle speed
n_f	number of elements
n_p	angular traverse speed along the tool path
N	number of flutes
q	element number

R_s	radius of the slot
R_c	radius of the cutter
s_t	feed rate
t	time
t_{local}	local time in an element
T_s	spindle period
T_p	period of tool's planetary motion
t_c	time in cut
t_f	time spent during not cutting
w	number of revolutions
z	axial elevation
α_{ij}	directional coefficients ($i, j = x, y, z$)
β	helix angle
ξ_x	damping ratio
ε	phase shift between two waves
ψ	phase shift
γ_i	trial functions ($i=1,2,3,4$)
η_p	test functions ($p=1,2$)
$\Delta x, \Delta y, \Delta z$	vibrations in x, y and z directions
Δu	vibrations in chip thickness direction
Λ	eigenvalue
Λ_I, Λ_R	imaginary and real part of eigenvalue

$[\Phi]$	transfer function matrix
$Re(\Phi)$	real part of the transfer function
$Im(\Phi)$	imaginary part of the transfer function
Φ_0	oriented transfer function
Φ_{xx}, Φ_{yy}	direct transfer function in x and y directions
θ	tool center position
ϕ_{st}, ϕ_{ex}	cutter entry and exit angles
ϕ_p	pitch angle
ϕ	instantaneous immersion angle
ϕ_j	immersion angle
ϕ_0	geometric mean of immersion angle
τ	time delay and tooth passing period
ω	angular velocity of the tool
Ω	angular velocity of the tool around the workpiece
ω_n	natural frequency
ω_c	chatter frequency
ω_τ	tooth passing frequency

Chapter 1

Introduction

Milling is one of the most common metal cutting processes in the aerospace and die & mold industries to produce wide variety of shapes from flat to angular and freeform surfaces. Periodic milling forces may cause deflections on the workpiece which lead to poor and wavy surface finish. The aim of the manufacturing research is to understand, model and predict the parameters which influence the surface quality, dimensional accuracy, machining cycle time and the cost which are important criteria in industry. The problems caused by periodic cutting forces and chatter vibrations can be avoided by selecting conservative depth of cut and spindle speed values and by increasing the dynamic stiffness of the machine tool-workpiece structure. However, such solutions result higher cost and loss in productivity. On the other hand, the process parameters can be optimized by mathematically modeling the interaction between the machine tool structure, workpiece, tool, cutting conditions and the machining process.

Circular milling operation is a new machining strategy to empty pockets in die and mold industry, and to remove excess material from solid blanks to produce monolithic parts in the aerospace industry. In regular milling operation, the tool follows a straight or curved path with a constant immersion as long as the geometry of the workpiece remains constant along the tool path. In circular milling, the tool follows a circular trajectory in a plane. Due to kinematics of circular milling, the radial width of cut changes continuously which leads to time varying chip loads. Variation in chip load causes time and cutter position dependent periodic cutting forces in circular milling. Time varying chip loads may cause shifts in chatter stability lobes to higher axial depth of cut values for a given spindle speed value. The aim of this thesis is to model the mechanics and dynamics of circular milling operation which leads to the prediction of cutting forces and the chatter stability of the system.

The thesis is organized as follows:

Chapter 2 covers the necessary background and the review of literature in milling process. Fundamentals of milling operation, previous models for prediction of cutting forces and chatter stability models are reviewed.

Chapter 3 is dedicated to the mechanics of circular milling operations. Mechanics of circular milling is modeled. The generated static cutting forces are predicted and verified experimentally.

In Chapter 4, an alternative numerical stability method, so-called the Direct Method, proposed by Sipahi et al. [31] for the stability analysis of linear time invariant time delay systems is presented. The chatter stability of single degree of freedom milling system is investigated by using the Direct method. The stability lobes simulated by using the Direct method is compared with the analytical, frequency domain solution presented by Altintas and Budak [11, 12]. The advantages and disadvantages of the Direct method are discussed.

Dynamics of circular milling operation is explained in Chapter 5. Chatter stability of circular milling process is solved by implementing two different analytical solutions. The frequency domain solution proposed by Altintas and Budak [11, 12] and time finite element analysis introduced by Bayly et al. [7, 8] are applied. Chatter stability lobes are predicted and compared against the experimental results.

The thesis is concluded with a summary of the performed study and possible future research directions.

Chapter 2

Literature Review

2.1. Introduction

Since milling operations are widely used in the manufacturing industry, significant research has been reported in the literature which is reviewed in this chapter.

2.2. Mechanics of Milling Operation

Milling operation is an interrupted cutting process in which more than one point of the tool is contact with the workpiece. The workpiece is clamped on table and fed towards the rotating cutter with N number of flutes placed in a rotating spindle (See Figure 2.1).

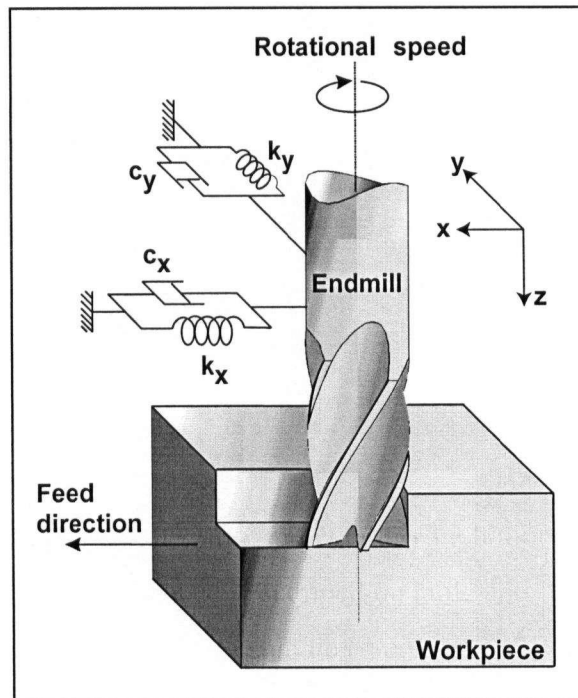


Figure 2.1 : Milling operation

Unlike in the turning process, chip thickness changes continuously during milling operation due to rotation of the tool. Milling operation is classified into two groups namely face and periph-

eral (end) milling. In face milling operations, the entry ϕ_{st} and exit ϕ_{ex} angles of the tool are different from zero (See Figure 2.2). There are two types of peripheral milling operation: conventional (up) and climb (down) milling. The entry angle ϕ_{st} is zero and exit angle ϕ_{ex} is different from zero in up milling operations. Thickness of the chip is zero at the beginning and increases as the tool rotates. The case is vice versa of up milling in down milling. The chip thickness takes its maximum value when the tool enters the workpiece and approaches to zero at the end of down milling operation. Since the cutting forces are a function of the chip thickness, the chip thickness generation is the main subject of early research [1, 9, 10, 28, 30]. Martellotti [22, 23] showed that actual path of the flute is an arc of trochoid and therefore the chip thickness has a complicated definition. He approximated the chip thickness h when the radius of the tool is larger than feed rate as follows:

$$h = s_f \sin \phi \quad (2.1)$$

where

s_f is the feed rate and ϕ represents the instantaneous immersion angle. (See Figure 2.2) When the dynamics of milling operation such as vibrations and tool jumping out of cut is considered, the chip thickness expression given by Equation (2.1) can not explain the true kinematics. Altintas et al. [14, 21, 26] developed a more accurate kinematic model in time domain which digitizes the cutting surface and tool locations. The previously and presently cut surfaces are divided into small segments and by taking the difference between the two at each time step, more accurate chip thickness is evaluated. The model covers both the dynamics of the machine tool-workpiece structure and the kinematics of chip formation.

Cutting forces are dependent not only the chip thickness but also axial depth of cut and cutting constants. The previous researchers, Tlusty&McNeil [35], Kline et al. [17], Sutherland and DeVor [32], and Montgomery and Altintas [26], focused on the relation between the cutting forces and cutting conditions. Armarego&Epp [6] developed a linear edge force model which is used in this thesis in order to calculate the cutting forces.

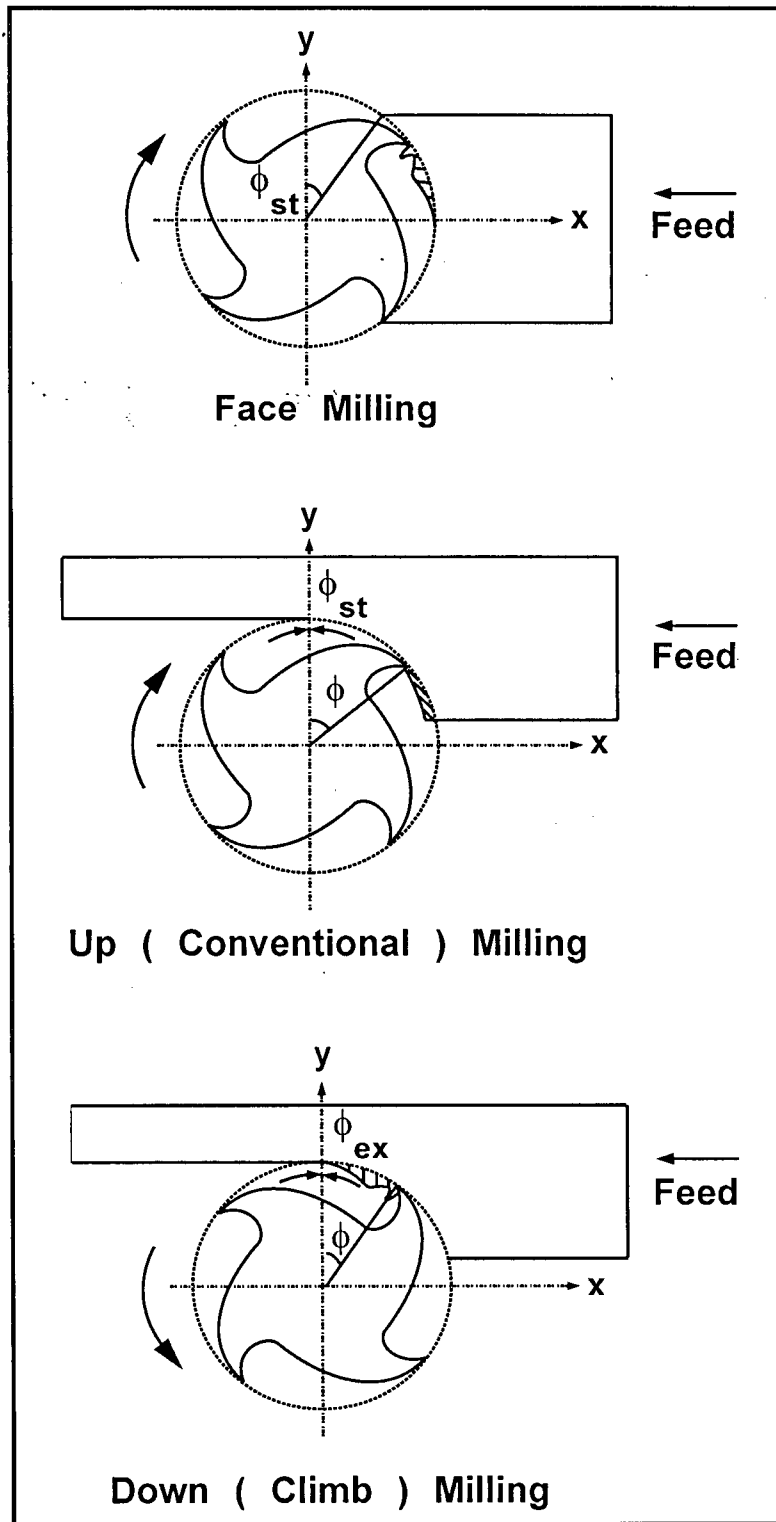


Figure 2.2 : Face, up and down milling

In the model, cutting forces are defined in terms of axial depth of cut b , chip thickness h and cutting constants K_c, K_e :

$$F = K_c b h + K_e b \quad (2.2)$$

Cutting constants K_c, K_e are evaluated through either orthogonal to oblique transformation or using the mechanistic model [2, 17, 32, 35, 36].

In the orthogonal to oblique transformation cutting, the cutting velocity is straight. (See Figure 2.3) The cutting coefficients (K_c, K_e) are expressed in terms of tool geometry (rake and helix angles) and material properties (friction angle, shear angle and shear stress) [13]. The method is applicable when the cutting edge is sharp and the rake face of the tool is smooth.

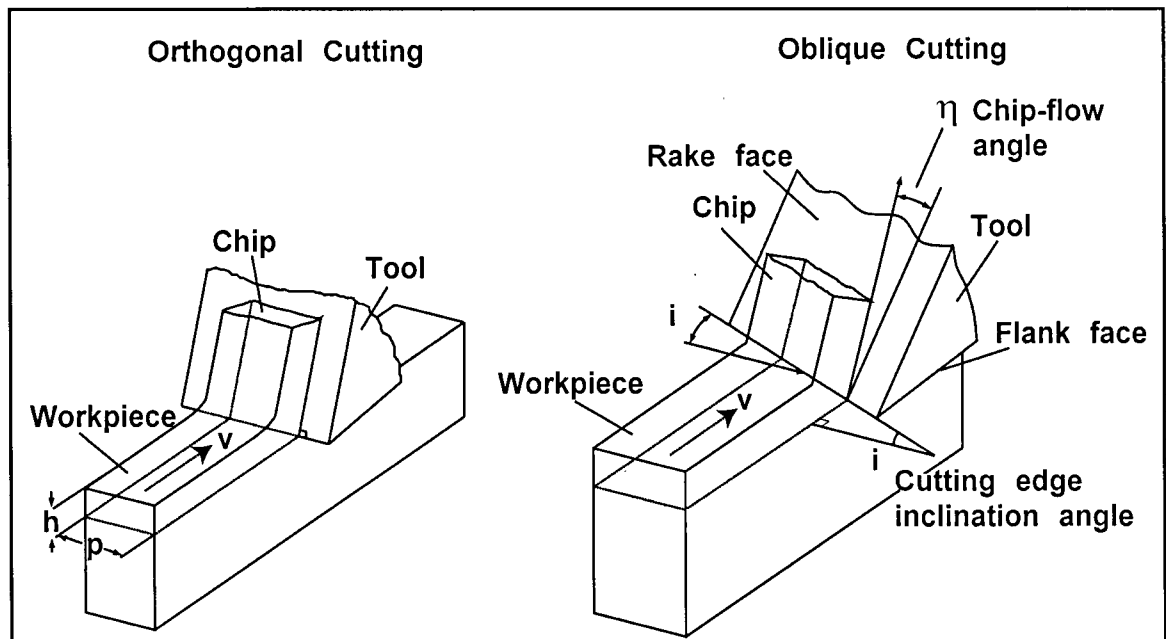


Figure 2.3 : Orthogonal and oblique cutting operations

Mechanistic model studied by Thusty&McNeil [35], Kline et al. [17], Sutherland and DeVor [32], and Montgomery and Altintas [26], is more practical when the cutting edge has a very complex geometry. A set of milling experiments are conducted for specified workpiece material and tool geometry at different feed rates (s_f) and the cutting forces are measured. Axial depth of cut b and radial width of cut (immersion) are kept constant during the operation. By fitting a linear relationship to the experimental cutting force data as expressed in Equation (2.2), the average cutting coefficients K_c, K_e are identified.

2.3. Dynamics of Milling Operation

When the vibrations of the machine tool-workpiece structure and its interactions with the cutting process are included, the process becomes dynamic. When the process becomes unstable, dynamic chatter vibrations occur which is one of the most severe problems in hindering productivity in industry. Chatter, a self excited vibration, can be best explained by the "regeneration of waviness" phenomenon. When there is a relative vibration between tool and workpiece, the flute in cut generates undulations on the finished surface. The succeeding flute which also vibrates, cuts and leaves wavy surfaces. (See Figure 2.4) The chip removed by the succeeding flute has a dynamic thickness because of the waviness on both sides of the chip. The dynamic chip thickness and hence the cutting forces may exponentially grow depending on the phase shift between the two subsequent waves while the machine tool-workpiece structure oscillates. Since the chatter is dependent on preceding pass of the flute, equation of motion of the milling operation has a time delay (τ) term. The fundamental parameters, which affect the stability of dynamic cutting process are the time delay (i.e. period of the tooth evaluated from the spindle speed) and depth of cut. Unless avoided, chatter leads to large growing dynamic cutting forces that cause poor surface finish and may damage the machine.

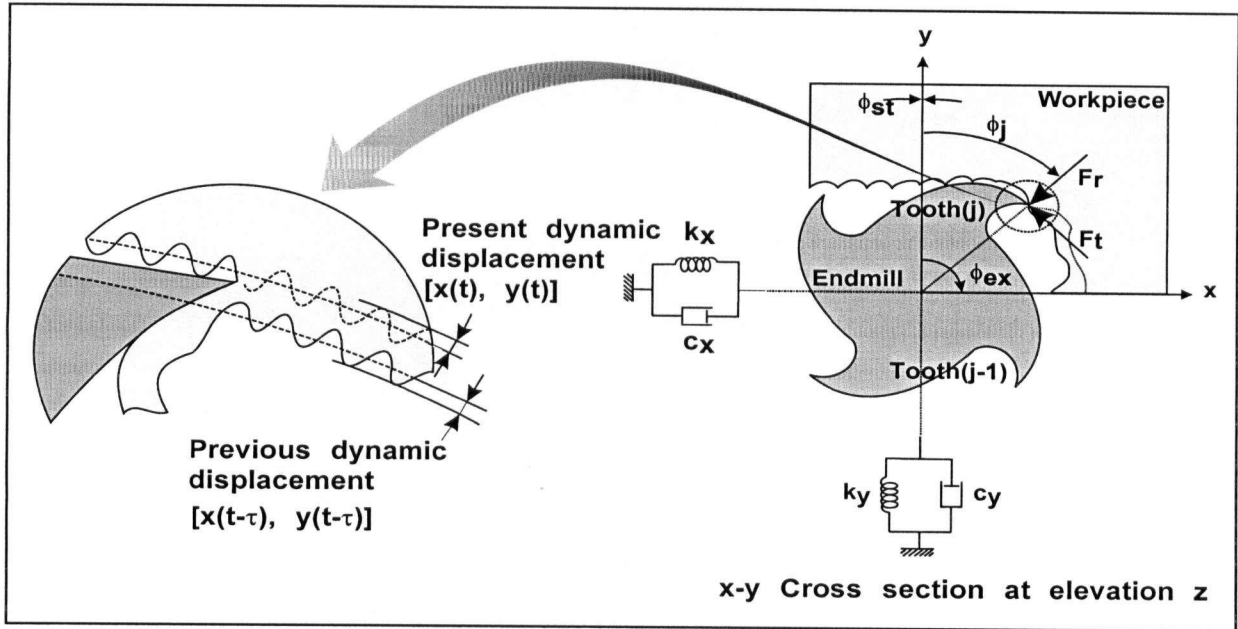


Figure 2.4 : Dynamic chip generation in milling

Tlusty [34] and Tobias [39] were the first researchers who studied the dynamics of the machining operations and explained chatter theory by regeneration phenomenon. Merritt [24] verified the theory by using feed back control theory. The developed chatter stability theory is mainly valid for orthogonal cutting process in which the directions of cutting forces and excitation are constant. (See Figure 2.5)

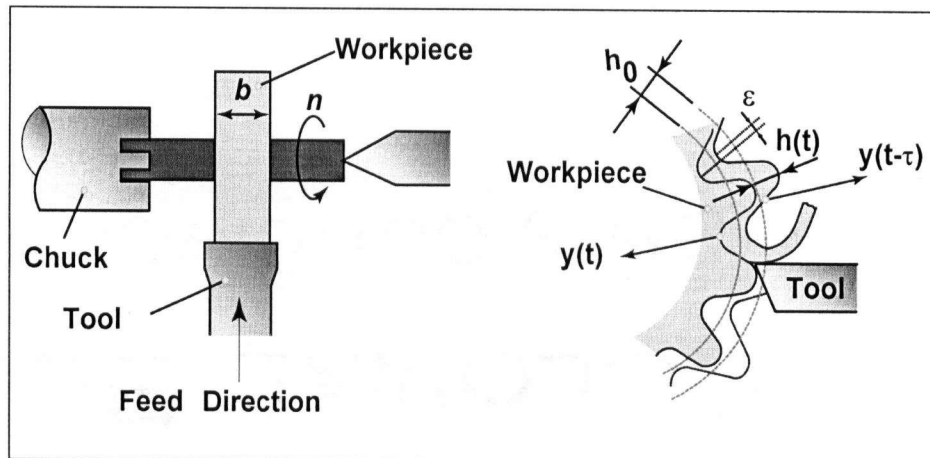


Figure 2.5 : Regeneration mechanism in orthogonal cutting

The model for chatter stability of milling operation is more complicated because of rotation of the tool with multiple flutes and coupled dynamics of the machine in orthogonal directions. Unlike in single point cutting, directional milling coefficients that determine the directions of cutting forces and excitation are time dependent.

Assume that there is only one tooth which is at the radial immersion position ϕ measured clockwise from the y axis. The feed direction is aligned with the x axis of the machining system. Neglecting the axial force for simplicity, there are two rotating force vectors acting on the tooth, tangential force F_t and radial force F_r (See Figure 2.4), which are expressed as follows [11, 12]:

$$\begin{aligned} F_t &= K_{tc}bh(\phi) \\ F_r &= K_r F_t = K_r K_{tc}bh(\phi) \\ \theta &= \text{atan} \frac{F_r}{F_t} = \text{atan} K_r \end{aligned} \quad (2.3)$$

where K_r is the ratio of radial to tangential cutting forces. The resultant cutting force on the tooth becomes:

$$F(\phi) = K_{tc}\sqrt{1+K_r^2}bh(\phi) = K_sbh(\phi) \quad (2.4)$$

where the resultant cutting force coefficient is $K_s = K_{tc}\sqrt{1+K_r^2}$. When the tool has an approach angle, a three dimensional model of the milling force must be considered with a more detailed milling model as presented by Altintas [4]. The cutting forces in the feed and normal directions can be resolved as follows:

$$F_x(\phi) = -F\cos(\phi - \theta), \quad F_y(\phi) = F\sin(\phi - \theta) \quad (2.5)$$

The dynamic chip load created by the tooth and vibrations is [11, 12]:

$$h(\phi) = s_t \sin \phi + \Delta x(t) \sin \phi + \Delta y(t) \cos \phi \quad (2.6)$$

where $\phi = \omega t$ is the angular position of the tooth for a spindle speed of ω [rad/s]. Note that the static chip load $s_t \sin \phi(t)$ is an input to the closed loop dynamics of the chatter, and does not affect the critical stability of the linear, dynamic machining system. Both vibration components $(\Delta x, \Delta y)$ are dominated by the chatter vibration frequency (ω_c); so as the resultant cutting force, e.g. $F(t) = F e^{i\omega_c t}$. The vibrations at present t (x, y) and previous tooth period $t - \tau$ (x_0, y_0) can be expressed by [3]:

$$\begin{aligned} x &= \Phi_{xx}(i\omega_c)F_x(\omega_c), & x_0 &= e^{-i\omega_c \tau} \Phi_{xx}(i\omega_c)F_x(\omega_c) \\ y &= \Phi_{yy}(i\omega_c)F_y(\omega_c), & y_0 &= e^{-i\omega_c \tau} \Phi_{yy}(i\omega_c)F_y(\omega_c) \\ \Delta x &= x - x_0, & \Delta y &= y - y_0 \end{aligned} \quad (2.7)$$

where Φ_{xx} and Φ_{yy} are direct frequency response functions (FRF) of the structure in x and y directions, respectively. Since the cutting forces F_x and F_y are both dependent on the vibrations in the directions (x, y) , the system has coupled dynamics. The stability of milling had been advanced steadily by Tlusty [37, 38], Opitz [27], Minis & Yanushevsky [25], Altintas & Budak [11, 12] as reviewed by Altintas [5].

2.3.1. Tlusty's Approximate Solution

Tlusty simplified the process by orienting the cutting forces from the directions of orthogonal springs to the direction of resultant cutting force as follows [37, 38])

$$\begin{aligned}\Delta x &= (e^{-i\omega_c\tau} - 1)\Phi_{xx}(i\omega_c)\cos(\phi - \theta)Fe^{i\omega_c t} \\ \Delta y &= -(e^{-i\omega_c\tau} - 1)\Phi_{yy}(i\omega_c)\sin(\phi - \theta)Fe^{i\omega_c t}\end{aligned}\quad (2.8)$$

Substituting Equation (2.8) in the dynamic chip thickness Equation (2.6):

$$\begin{aligned}h(t) &= (e^{-i\omega_c\tau} - 1)[\sin\phi\cos(\phi - \theta) - \cos\phi\sin(\phi - \theta)]\begin{bmatrix} \Phi_{xx} \\ \Phi_{yy} \end{bmatrix}\{Fe^{i\omega_c t}\} \\ h(t) &= (e^{-i\omega_c\tau} - 1)[D(\phi)]\begin{bmatrix} \Phi_{xx} \\ \Phi_{yy} \end{bmatrix}\{Fe^{i\omega_c t}\}\end{aligned}\quad (2.9)$$

The formulation given here orients vibrations and cutting forces from x, y spring directions to the direction of chip load ϕ . $D(\phi)$ is a periodic function and valid only between the entry ϕ_{st} and exit angles ϕ_{ex} of cut. Tlustý used geometric mean of the immersion angle [37] (See Figure 2.6), rather than taking an average value of $[D(\phi)]$ as used by Opitz [27] and Weck [41] as:

$$\phi_0 = \phi_{st} + \frac{\phi_{ex} - \phi_{st}}{2}\quad (2.10)$$

The direction factors then become constant as:

$$u_x = \sin\phi_0\cos(\phi_0 - \theta), u_y = -\cos\phi_0\sin(\phi_0 - \theta)\quad (2.11)$$

which leads to time invariant and constant oriented frequency response function:

$$\Phi_{0,1} = u_x \Phi_{xx} + u_y \Phi_{yy} \quad (2.12)$$

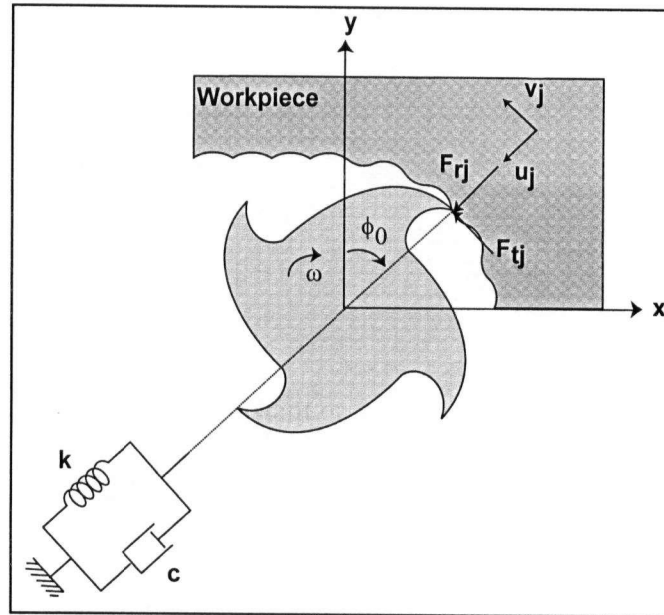


Figure 2.6 : Tlustý's stability model for half immersion up milling

2.3.2. Opitz's Approximate Solution

Unlike turning, the directional factors change as a function of spindle rotation, and they are periodic at cutter pitch angle $\phi_p = \frac{2\pi}{N}$. Opitz [27] used the average of the periodic directional function of the resultant force as opposed to geometric mean adopted by Tlustý.

$$\begin{aligned}
[D_0] &= \frac{1}{\phi_p} \int_{\phi_{st}}^{\phi_{ex}} [\sin\phi \cos(\phi - \theta) - \cos\phi \sin(\phi - \theta)] d\phi \\
[D_0] &= \frac{N}{2\pi} \left[\begin{array}{c} \frac{1}{2}(\sin\theta)\phi - \frac{1}{4}\cos(2\phi - \theta) \\ \frac{1}{2}(\sin\theta)\phi + \frac{1}{4}\cos(2\phi - \theta) \end{array} \right] \Bigg|_{\phi_{st}}^{\phi_{ex}} = \begin{bmatrix} v_x & v_y \end{bmatrix} \quad (2.13)
\end{aligned}$$

The oriented frequency response function of Opitz is also time invariant and constant, but different than Tlusty's approach.

$$\Phi_{0,2} = v_x \Phi_{xx} + v_y \Phi_{yy} \quad (2.14)$$

Weck [41] further considered the influence of direct and cross frequency response functions of the machine tool compliance similar to turning. However, while noting the time variation of the directional factors, he also averaged them and oriented all the vibrations at the cutting edge location. Hence, the time dependency from the chip thickness is still removed, and the chatter stability problem becomes a one-dimensional scalar problem since it is oriented in a fixed single direction like in turning. It can be solved by classical chatter theory presented earlier in 1950s by Tlusty [33] or Tobias [40]. The mean dynamic chip thickness becomes:

$$h_m = (e^{-i\omega_c \tau} - 1) \Phi_0 F e^{i\omega_c t} \quad (2.15)$$

The average of the periodic function corresponds to the average of the dynamic chip thickness, which leads to mean dynamic resultant cutting force,

$$Fe^{i\omega_c t} = K_s b h_m = K_s b (e^{-i\omega_c \tau} - 1) \Phi_0 F e^{i\omega_c t} \quad (2.16)$$

For critical borderline stability analysis, the characteristic equation of the dynamic milling becomes,

$$1 + (1 - e^{-i\omega_c \tau}) K_s b_{lim} \Phi_0(i\omega_c) \quad (2.17)$$

where b_{lim} is the maximum axial depth of cut for chatter vibration free machining. The stability lobes are then solved using the same formulation given for one dimensional theory [33, 40]:

$$b_{lim} = \frac{-1}{2K_s (Re(\Phi_0(\omega_c))) m_e} \quad (2.18)$$

$$\tau = \frac{2k\pi + \varepsilon}{\omega_c} \rightarrow n = \frac{60}{N\tau}$$

where ω_c [rad/sec] is the chatter frequency, τ [sec] is the tooth passing period, N is the number of teeth on the cutter, k is number of stability lobes and n [rev/min] is the spindle speed. $Re(\Phi_0)$ is the real part of the oriented frequency response function that can be evaluated by either approximations given in Equation (2.12) by Faassen [15] or in Equation (2.14) by Opitz [27]. Tlustý [37] adjusted the stability limit by scaling the system by an average number of teeth in cut, $m_e = \frac{N(\phi_{ex} - \phi_{st})}{2\pi}$. Since Opitz and Weck used the average resultant force direction by considering the pitch angle, $m_e = 1$ must be used in their models. The phase shift of the chatter waves can be found from:

$$\varepsilon = 3\pi + 2\psi \rightarrow \psi = \text{atan} \frac{Im(\Phi_0)}{Re(\Phi_0)} \quad (2.19)$$

The expression given in Equation (2.18) has been widely used as an extension of orthogonal chatter theory applied to milling.

Tobias [39, 40] invented the stability lobes by relating chatter free axial depth of cut b_{lim} with spindle speed n .

Averaging the time varying constants in direct and cross directions takes the maximum energy in exciting the structural modes, and the coupling between the vibrations in two directions via the cutting process is maintained by Altintas et al. [4]. The coupling treats the dynamic milling as an eigenvalue problem. Averaging the dynamic resultant force as proposed by Opitz [27], or forcing the resultant force to act at the geometric mean of the cut proposed by Tlustý [38] reduce the eigenvalue problem into a scalar one. Depending on the strength of modes in x and y directions, geometric averaging may shift the energy towards one direction more than the other, hence it may not lead to accurate results when the modes in both directions are equally strong or weak.

2.3.3. Altintas & Budak's Frequency Domain Solution

Floquet theory was used by Minis and Yanushevsky [25] to solve the stability of milling operation in frequency domain. An analytical method which considers the milling process as a two dimensional operation is developed by Budak & Altintas [11, 12]. They transformed the stability into an eigenvalue problem and solved it in frequency domain. They expressed chatter free axial depth of cut b_{lim} as follows:

$$b_{lim} = \frac{-2\pi\Lambda_R}{NK_{tc}} \left(1 + \left(\frac{\Lambda_I}{\Lambda_R} \right)^2 \right) \quad (2.20)$$

where K_{tc} is the cutting coefficient in tangential direction, Λ_R and Λ_I are the real and imaginary parts of the eigenvalue Λ , respectively. Eigenvalues Λ are calculated by taking the determinant of the characteristic equation of the milling system. Coupling between two orthogonal directions x and y is taken into account in this solution. Later, Altintas [4] extended the theory to three dimensions.

2.3.4. Bayly's Time Domain Solution

A new method, time finite element analysis, is used for the time domain stability of low immersion interrupted cutting operations by Bayly et al. [7]. The system was assumed to be a single degree of freedom system. The interrupted cutting operation was investigated in two parts, namely cutting (forced vibration) and not cutting (free vibration). They divided the time in cut into finite elements and estimated displacement on each element during w^{th} pass of the flute as follows:

$$\ddot{x}(t) = \sum_{i=1}^4 \ddot{a}_{qi}^w \cdot \gamma_i(t_{local}) \quad (2.21)$$

where $\gamma_i(t_{local})$ are trial functions, cubic Hermite polynomials, \ddot{a}_{qi} are coefficients of the trial functions used for position and velocity boundary conditions of the elements and t_{local} is the local time on q^{th} element. Single degree of freedom interrupted cutting operation (turning) is shown in Figure 2.7:

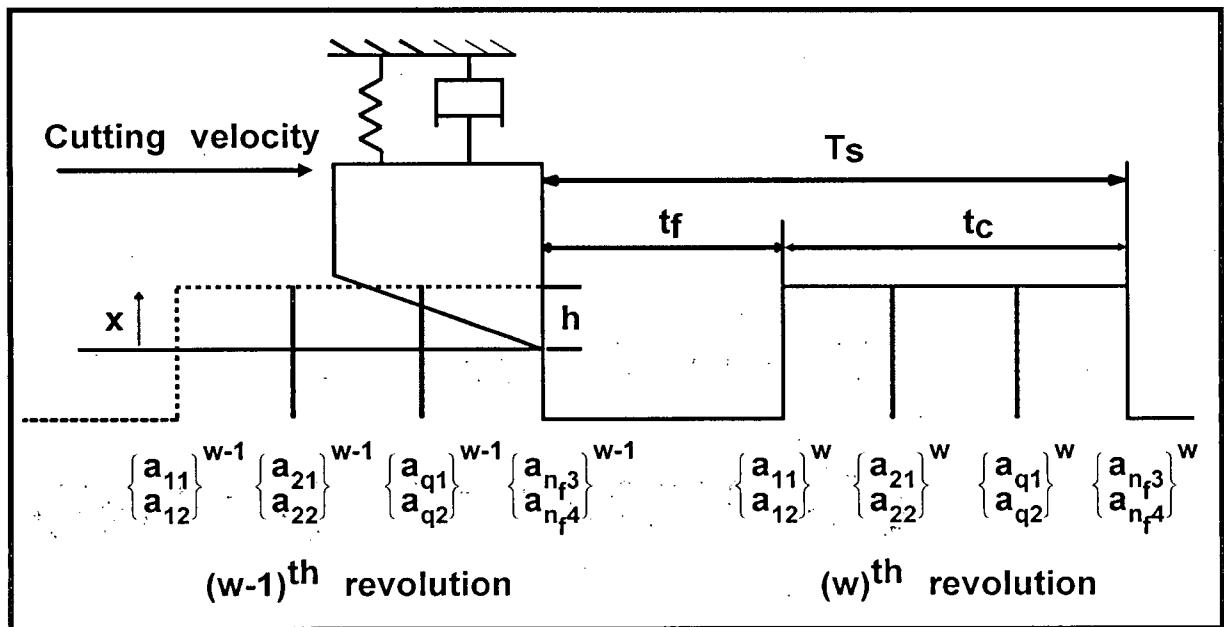


Figure 2.7 : Single degree of freedom interrupted turning model

where T_s is spindle period, t_c defines time spent in cut, $t_f = T_s - t_c$ shows time spent during not cutting.

Boundary conditions between elements were set by equating the displacement and velocity at the end of each element with the displacement and velocity at the beginning of the next element. The interrupted cutting operation is modeled as a discrete system. Equation of motion of the discrete system is rearranged in order to express the coefficients of the estimated displacement expression of an element at current pass $\hat{a}_{q_i}^w$ in terms of the coefficients at previous pass $\hat{a}_{q_i}^{w-1}$ and intended chip thickness h_{int} :

$$\hat{a}^w = [Q]\hat{a}^{w-1} + [S] \quad (2.22)$$

Magnitudes of the eigenvalues of $[Q]$ matrix are determined for stability analysis of the discrete system. If the magnitudes are within the unit circle, the cutting is stable, and it is unstable otherwise.

Later, Bayly's et al. [8] extended their work to two degrees of freedom interrupted systems. Two dimensional low immersion milling was used as an example. The rotation of the cutting forces in milling operation was considered as a function of immersion angle. The equation of motion was written in matrix-vector form in order to extend the model for multi degrees of freedom systems easily. The time finite element method is explained in detail in Chapter 5.

Time finite element method gives accurate results for low immersion interrupted cutting operations. The displacement and cutting forces can be simulated by using time finite element method but can not be predicted by frequency domain solution introduced by Altintas et al. [11, 12].

2.3.5. Solution of a Linear Time Invariant Systems with a Time Delay

Sipahi et al. [31] presented an analytical solution for the stability of linear time invariant time delay systems. Time delay τ in the equation of motion makes the system nonlinear. In order to

eliminate the nonlinearity, they replaced the time delay term $e^{-\tau s}$ in the characteristic equation with a bilinear expression [29])

$$e^{-\tau s} = \frac{1 - Ts}{1 + Ts} \quad (2.23)$$

The solution is exact when the system is critically stable. They checked the stability of the new characteristic equation of the system by using Routh Hurwitz array. The details of the method and its application to milling system is explained in Chapter 4.

Chapter 3

Mechanics of Circular Milling

3.1. Introduction

Circular milling is used for removing excess material from workpiece such as enlarging holes and forming slots in industry. The tool is following a circular toolpath in xy plane while the workpiece is being fed towards the tool as shown in Figure 3.1

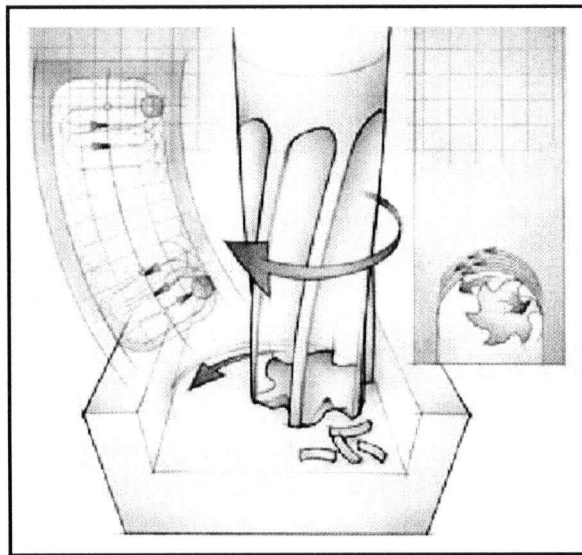


Figure 3.1 : Formation of a slot by using circular milling (Source: Sandvik Coromant)

The process is completed in xy plane with a constant axial depth of cut, followed by axial plunging to the workpiece at a fixed increment followed by circular milling again. As the tool travels around the circular path, the intersection of tool and workpiece changes as shown in Figure 3.2.

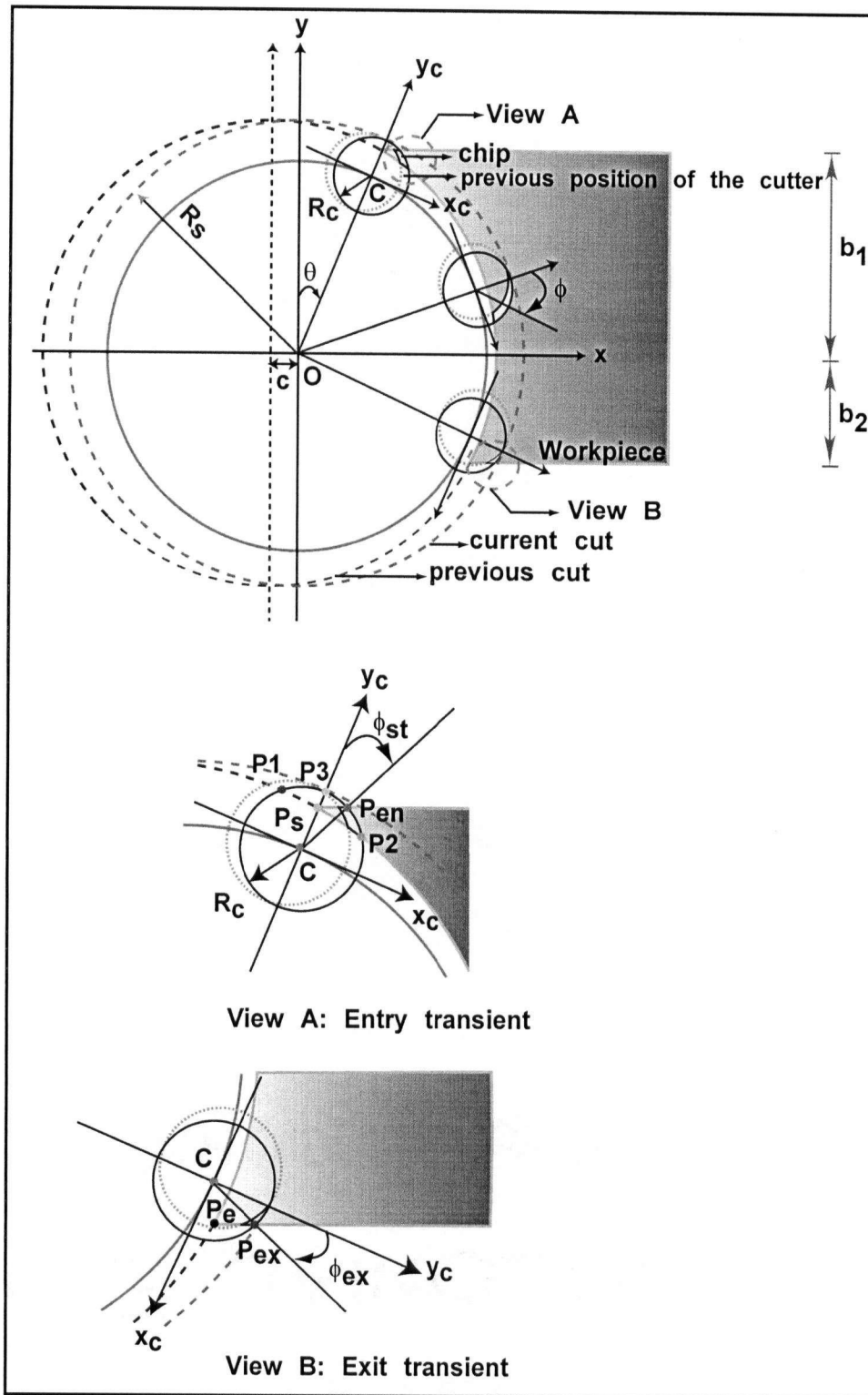


Figure 3.2 : Top view of circular milling

The tool follows a trochoidal trajectory [22,23,26], and has a time varying orientation along the cut which determines variation in chip load and the cutting forces. Circular milling operation is studied in three different zones shown in Figure 3.2 namely entry transient, steady state and exit transient zones. In this chapter, mathematical modeling of the tool-workpiece intersection is explained; prediction of cutting forces is discussed and consequently experimental validation of the mathematical model by using Al7075-T6 is given.

3.2. Geometric Modeling of Tool and Workpiece Intersection

The entry ϕ_{st} and exit ϕ_{ex} angles of the tool, which change continuously in circular milling, must be identified to predict the chip load as well as the cutting forces. The entry ϕ_{st} and exit ϕ_{ex} angles are evaluated from the geometric intersection of tool and circular slot, which needs to be milled. The coordinates of a point P on the tool and on the previous path measured from the current circular trajectory center O can be expressed as (See Figure 3.2):

$$\begin{aligned} (x - (R_s - R_c) \sin \theta)^2 + (y - (R_s - R_c) \cos \theta)^2 &= R_c^2 \\ (x + c)^2 + y^2 &= R_s^2 \end{aligned} \quad (3.1)$$

The upper and lower boundaries of the workpiece are given as:

$$y = b_1 \quad y = -b_2 \quad (3.2)$$

The local immersion angle ϕ is measured in clockwise direction from the (y_c) axis normal to the finish surface in tool coordinates. The tool may enter the workpiece with non-zero entry angle ϕ_{st} if the upper width of cut is less than the radius of the slot, i.e. ($b_1 < R_s$) as shown in Figure 3.2. As soon as the tool enters the workpiece at point P_{en} , the entry angle of the tool will approach towards zero ($\phi_{st} = 0$) after a short transient phase (entry transient zone), but the exit angle ϕ_{ex} will vary as the tool - slot intersection point changes its coordinates with the tool center posi-

tion, $\theta = \theta(t)$. By substituting Equation (3.2) into the previous slot trajectory expression in Equation (3.1), the intersection of the previous tool path and workpiece boundaries can be evaluated at the entry P_s and exit P_e points respectively (See Figure 3.2.) Out of two solutions, the one which has positive x leads to the desired intersection points as follows:

$$(x_s, y_s) = (-c + \sqrt{R_s^2 - b_1^2}, b_1) \quad (3.3)$$

$$(x_e, y_e) = (-c + \sqrt{R_s^2 - b_2^2}, -b_2) \quad (3.4)$$

In the following subsections, the entry ϕ_{st} and exit ϕ_{ex} angles are expressed in the entry transient, steady state and exit transient zones.

$y_C \geq b_1 + R_c$ not cutting

$y_C > b_1 - R_c$ and $x_{en} \leq x_s$ not cutting

$y_C > b_1 - R_c$ and $x_{en} > x_s$ Entry transient zone

$(y_3 \leq b_1$ and $x_e \geq x_{ex}) \rightarrow \phi_{st} = 0$ Steady state zone

$y_3 \leq b_1$ and $x_e < x_{ex}$ Exit transient zone

$y_3 = b_2$ end of cutting

Here, the sub-indices of each coordinate indicates the point (P) they belong to.

3.2.1. Entry Transient Zone ($y_3 > b_1$):

The tool enters the workpiece at point P_{en} , and its coordinates are given by substituting $(y = b_1)$ into the tool expression given in Equation (3.1).

$$(x_{en}, y_{en}) = \left(\frac{-c_1 + \sqrt{c_1^2 - 4c_2c_0}}{2}, b_1 \right) \quad (3.5)$$

where

$$c_2 = 1$$

$$c_1 = -2(R_s - R_c)\sin\theta$$

$$c_0 = R_s^2 - 2R_sR_c + b_1^2 - 2(R_s - R_c)b_1\cos\theta$$

The larger of the two solutions from Equation (3.5) yields the x coordinate of the entry point P_{en} . By substituting the expression for the previous slot trajectory ($y^2 = R_s^2 - (x + c)^2$) given in Equation (3.1) into the tool expression in Equation (3.1), their intersection points $P_1(x_1, y_1)$ and $P_2(x_2, y_2)$ can be found as a function of the step over feed c and angular position of the tool θ with respect to circular slot center (O):

$$x = Ay + B \quad (3.6)$$

where

$$A = -\frac{2(R_s - R_c)\cos\theta}{2c + 2(R_s - R_c)\sin\theta}$$

$$B = -\frac{2R_s^2 - c^2 + 2R_sR_c}{2c + 2(R_s - R_c)\sin\theta}$$

By substituting x into the previous trajectory expression in Equation (3.1):

$$\begin{aligned} y^2 &= R_s^2 - (Ay + B + c)^2 \\ a_2y^2 + a_1y + a_0 &= 0 \end{aligned} \quad (3.7)$$

where

$$a_2 = A^2 + 1$$

$$a_1 = 2AB + 2Ac$$

$$a_0 = B^2 + 2Bc + c^2 - R_s^2$$

The quadratic equation has two roots which yields two intersection points $P_1(x_1, y_1)$ and $P_2(x_2, y_2)$ between the tool and circular slot segment (See Figure 3.2):

$$(x_{1,2}, y_{1,2}) = Ay_{1,2} + B, \frac{-a_1 \pm \sqrt{\Delta}}{2a_2} \quad (3.8)$$

where

$$\Delta = a_1^2 - 4a_2a_0$$

The tool does not cut any material behind its front periphery, hence the chip is not generated between $P_1(x_1, y_1)$ and $P_3(x_3, y_3)$ (See Figure 3.2). The tool starts entering the work material at $P_3(x_3, y_3)$ and exits at $P_2(x_2, y_2)$ point . The coordinates of the tool center C and entry point P_3 can be expressed in global slot coordinates as:

$$\begin{aligned} (x_3, y_3) &= (R_s \sin \theta, R_s \cos \theta) \\ (x_c, y_c) &= ((R_s - R_c) \sin \theta, (R_s - R_c) \cos \theta) \end{aligned} \quad (3.9)$$

A triangle is formed by $P_{en}(x_{en}, y_{en})$, $P_3(x_3, y_3)$, $C(x_c, y_c)$ on the tool and the entry angle of the tool ϕ_{st} into the workpiece at point $P_{en}(x_{en}, y_{en})$ is evaluated parametrically as:

$$\phi_{st} = \text{acos} \left(\frac{L_{enC}^2 + L_{3C}^2 - L_{en3}^2}{2L_{enC}L_{3C}} \right) \quad (3.10)$$

where

$$L_{3C} = \sqrt{(x_3 - x_C)^2 + (y_3 - y_C)^2}$$

$$L_{enC} = \sqrt{(x_{en} - x_C)^2 + (y_{en} - y_C)^2}$$

$$L_{en3} = \sqrt{(x_{en} - x_3)^2 + (y_{en} - y_3)^2}$$

From the triangle connecting points $P_3(x_3, y_3)$, $C(x_C, y_C)$, $P_2(x_2, y_2)$, the exit angle of the tool ϕ_{ex} at point $P_2(x_2, y_2)$ can be calculated as:

$$\phi_{ex} = \arccos\left(\frac{L_{2C}^2 + L_{3C}^2 - L_{23}^2}{2L_{2C}L_{3C}}\right) \quad (3.11)$$

where

$$L_{2C} = \sqrt{(x_2 - x_C)^2 + (y_2 - y_C)^2}$$

$$L_{23} = \sqrt{(x_2 - x_3)^2 + (y_2 - y_3)^2}$$

Points $P_3(x_3, y_3)$, $C(x_C, y_C)$, $P_2(x_2, y_2)$ are expressed parametrically as a function of tool's angular position θ in Equations (3.8) and (3.9). By incrementing (θ) at discrete intervals, the variation of entry ϕ_{st} and exit ϕ_{ex} angles can be evaluated from Equations (3.10) and (3.11).

3.2.2. Steady State Zone ($y_3 \leq b_1$ and $x_e \geq x_{ex}$):

As the tool enters the steady state zone ($y_3 = b_1$) the entry angle ϕ_{st} becomes zero and during the rest of the cutting operation the entry angle ϕ_{st} is always zero. The exit angle ϕ_{ex} can be evaluated as:

$$\phi_{st} = 0$$

$$\phi_{ex} = \arccos\left(\frac{L_{2C}^2 + L_{3C}^2 - L_{23}^2}{2L_{2C}L_{3C}}\right) \quad (3.12)$$

3.2.3. Exit Transient Zone ($y_3 \leq b_1$ and ($x_e < x_{ex}$)):

The entry angle ϕ_{st} is always zero in this zone, while the exit angle ϕ_{ex} decreases which is shown at point $P_{ex}(x_{ex}, y_{ex})$. (Figure 3.2) By substituting ($y = -b_2$) to the tool expression in Equation (3.1), the x coordinate of the exit point can be evaluated as:

$$(x_{ex}, y_{ex}) = \left(\frac{-d_1 + \sqrt{d_1^2 - 4d_2d_0}}{2}, -b_2 \right) \quad (3.13)$$

where

$$d_2 = 1$$

$$d_1 = -2(R_s - R_c)\sin\theta$$

$$d_0 = R_s^2 - 2R_sR_c + b_1^2 + 2(R_s - R_c)b_2\cos\theta$$

The expression for the varying exit angle ϕ_{ex} as the tool leaves the workpiece can be evaluated from the triangle $P_3(x_3, y_3)$, $C(x_C, y_C)$, $P_{ex}(x_{ex}, y_{ex})$:

$$\phi_{st} = 0, \quad \phi_{ex} = \arccos\left(\frac{L_{exC}^2 + L_{3C}^2 - L_{ex3}^2}{2L_{exC}L_{3C}}\right) \quad (3.14)$$

where

$$L_{exC} = \sqrt{(x_{ex} - x_C)^2 + (y_{ex} - y_C)^2}$$

$$L_{ex3} = \sqrt{(x_{ex} - x_3)^2 + (y_{ex} - y_3)^2}$$

3.3. Cutting Force Formulation

The engagement conditions (ϕ_{st}, ϕ_{ex}) leads to the prediction of varying chip thickness h at each tool location (See Figure 3.3) as it rotates.

The spindle speed (n) and angular traverse speed along the tool path (n_p) in [rad/sec] are given as follows:

$$\omega = \frac{2\pi n}{60}, \Omega = \frac{2\pi n_p}{60} \quad (3.15)$$

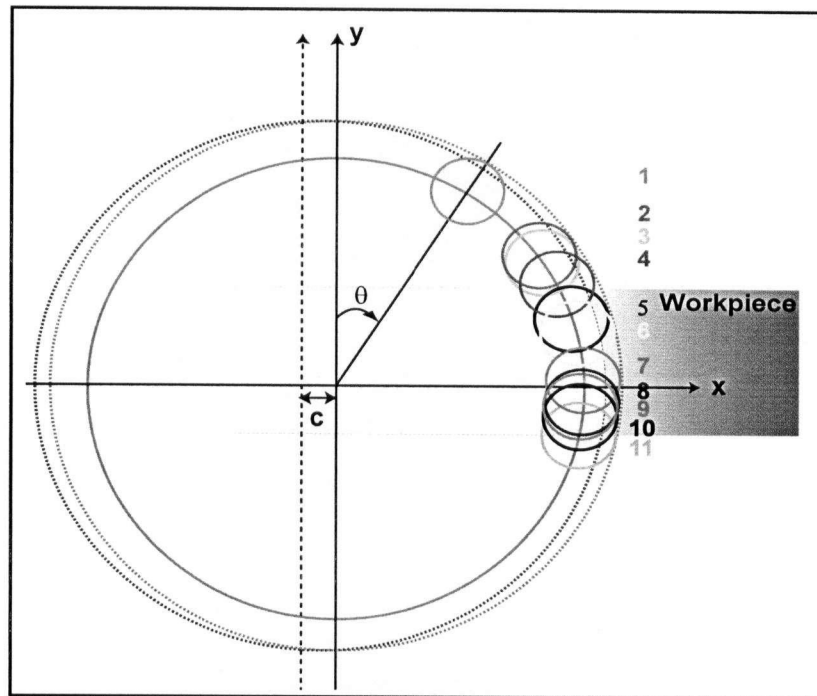


Figure 3.3 : Tool positions during operation

The feed f and feed rate s_t are measured along the feed axis of the tool (x_c), which is tangent to the circular tool path as shown in Figure 3.2 and given by:

$$\begin{aligned} f &= \Omega(R_s - R_c) \\ s_t &= f \frac{60}{Nn} \end{aligned} \quad (3.16)$$

The tool is traversed along the circular path at uniform, discrete time intervals (t):

$$\theta(k) = \theta_0 + \Omega kt, \quad \phi_1(k) = \phi_{10} + \omega kt \quad k = 0, 1, 2, \dots \quad (3.17)$$

θ_0 and ϕ_{10} are the initial positions of the tool and the first tooth respectively. The tool will be in the cutting zone and the tooth j will be cutting chip only if the following conditions are met:

$$\left(\frac{\pi}{2} - \text{asin} \frac{b_1}{R_s} \right) \leq \theta(k) \leq \left(\frac{\pi}{2} + \text{asin} \frac{b_2}{R_s} \right) \quad (3.18)$$

$$\phi_{st}(\theta) \leq \phi_j(k) \leq \phi_{ex}(\theta)$$

where the entry ϕ_{st} and exit ϕ_{ex} angles are identified along the path as given in the previous section. Otherwise the tooth will not cut any chip and contribute zero force to the process at that instance. Unless the width of cut varies, the process will be periodic both at the tooth passing frequency as well as at each frequency due to planetary motion.

As an example, a cylindrical endmill with N flutes and β helix angle is considered. The instantaneous immersion angle of tooth j , ϕ_j , at axial elevation z is expressed as (See Figure 3.4)

$$\phi_j(k) = \phi_1(k) + (j-1)\phi_p + z \frac{\tan \beta}{R_s} \quad (3.19)$$

The immersion dependent chip thickness h_j (Figure 3.1) cut by tooth j is given by:

$$h_j = s_t \sin \phi_j(k) \quad (3.20)$$

The tangential F_{tj} and radial F_{rj} forces (Figure 3.4) acting on the tooth j are:

$$\begin{bmatrix} F_{tj} \\ F_{rj} \end{bmatrix} = \begin{bmatrix} K_{tc}h_j + K_{te} \\ K_{rc}h_j + K_{re} \end{bmatrix} b \quad (3.21)$$

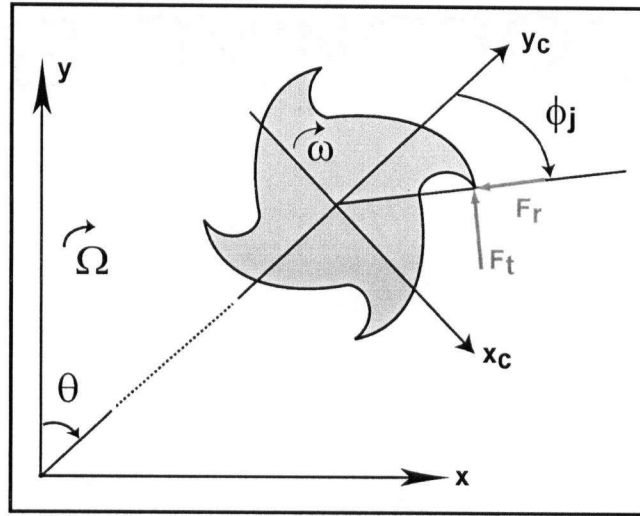


Figure 3.4 : Cutting forces in tangential and radial direction

By scanning all the teeth which are cutting the material, instantaneous cutting forces acting on them can be projected in the global coordinate system of the machine as follows:

$$\begin{aligned} F_x(\theta, \phi) &= \sum_{j=1}^N g(\phi_j) [(-F_{tj} \cos \phi_j - F_{rj} \sin \phi_j) \cos \theta + (F_{tj} \sin \phi_j - F_{rj} \cos \phi_j) \sin \theta] \\ F_y(\theta, \phi) &= \sum_{j=1}^N g(\phi_j) [(-F_{tj} \cos \phi_j - F_{rj} \sin \phi_j) \sin \theta + (F_{tj} \sin \phi_j - F_{rj} \cos \phi_j) \cos \theta] \end{aligned} \quad (3.22)$$

$$\begin{aligned} F_x(\theta, \phi) &= \sum_{j=1}^N g(\phi_j) [-F_{tj} \cos(\phi_j + \theta) - F_{rj} \sin(\phi_j + \theta)] \\ F_y(\theta, \phi) &= \sum_{j=1}^N g(\phi_j) [F_{tj} \sin(\phi_j + \theta) - F_{rj} \cos(\phi_j + \theta)] \end{aligned} \quad (3.23)$$

3.4. Simulations and Experimental Results

The circular milling algorithm presented in the thesis is experimentally verified with an end mill having $R_c = 10$ [mm] radius, $\beta = 30^\circ$ helix angle and $N = 4$ teeth. The cutting conditions were given as follows: the axial depth of cut $b = 2$ [mm], the step over feed $c = 0.9$ [mm]; the feed rate per tooth $s_t = 0.75$ [mm/rev/tooth]; the radial width of cut $b_1 = b_2 = 25$ [mm]; the radius of the slot $R_c = 10$; the spindle speed $n = 1000$ [rpm]; $n_p = 31.831$ [rpm]. The work material was selected Al7075-T6 with the cutting force coefficients of $K_{tc} = 796.077$ [N/mm²] and $K_{rc} = 168.829$ [N/mm²]. The edge force coefficients were $K_{te} = 27.711$ [N/mm] and $K_{re} = 30.801$ [N/mm].

The simulated and measured cutting forces in global coordinates are given in Figure 3.5 and Figure 3.6, respectively. The predicted cutting forces are in close agreement with the measurements. The normal forces, which represent tangential cutting force components, are largest when the tool is close to the center of the circular path ($\theta = \frac{\pi}{2}$). A detailed view of the predicted and the measured cutting forces is given in Figure 3.7. The slight difference may be due to poor synchronization of the measured and simulated forces, as well as slight errors in cutting force coefficients. Variation of exit angle ϕ_{ex} and chip thickness h due to the angular position of the tool θ are shown in Figure 3.8 and Figure 3.9. Exit angle ϕ_{ex} and chip thickness h take their maximum values near the circular slot center (O).

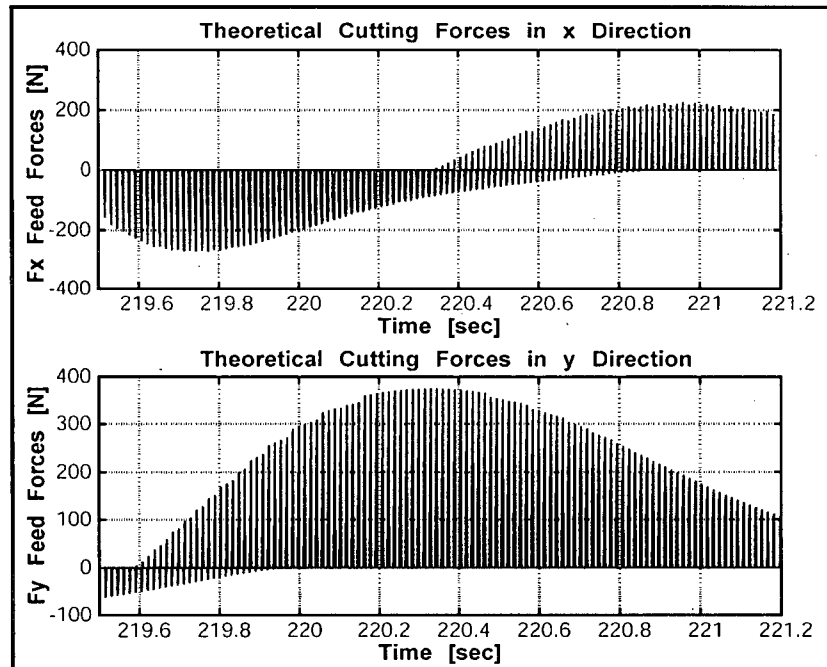


Figure 3.5 : Simulated cutting forces in x and y directions

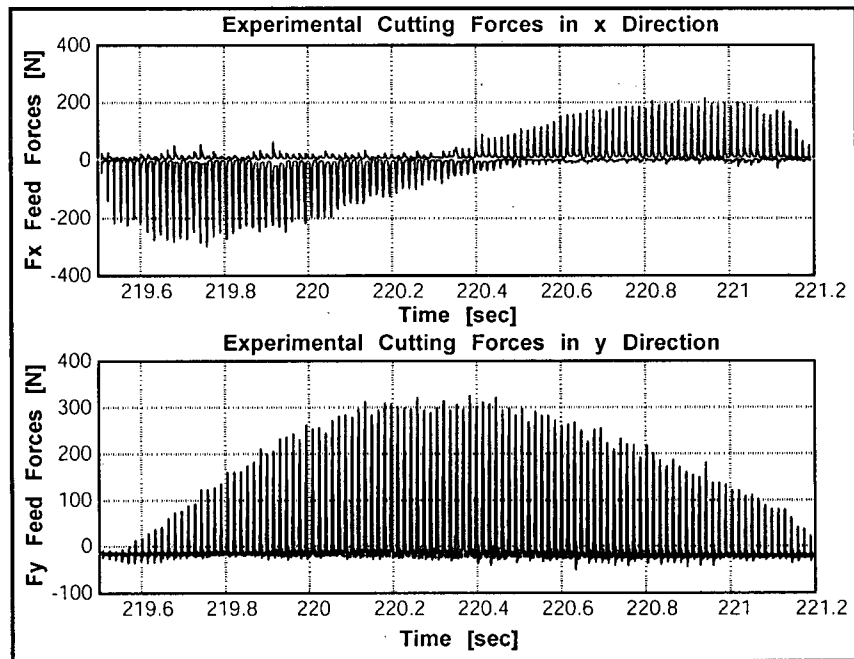


Figure 3.6 : Measured cutting forces in x and y directions

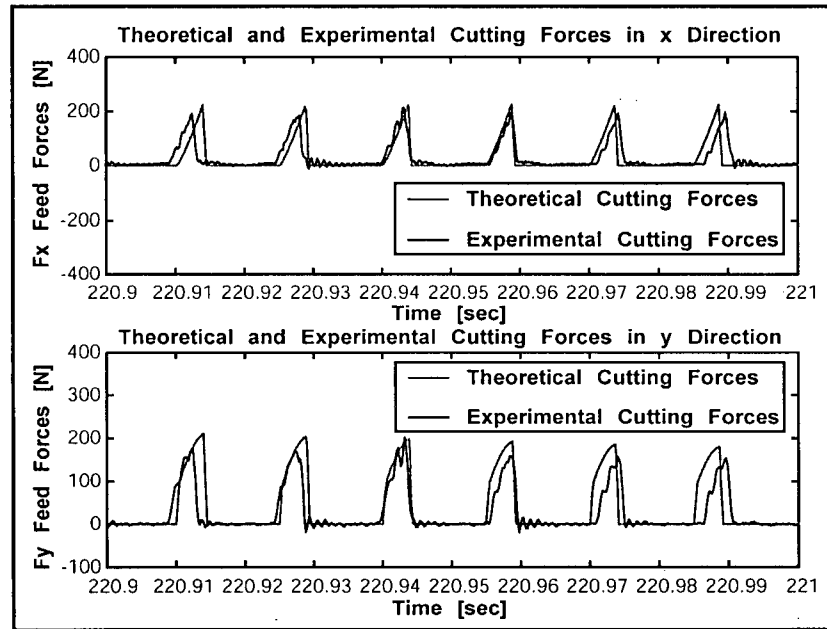


Figure 3.7 : Comparison of measured and simulated cutting forces at a small time window

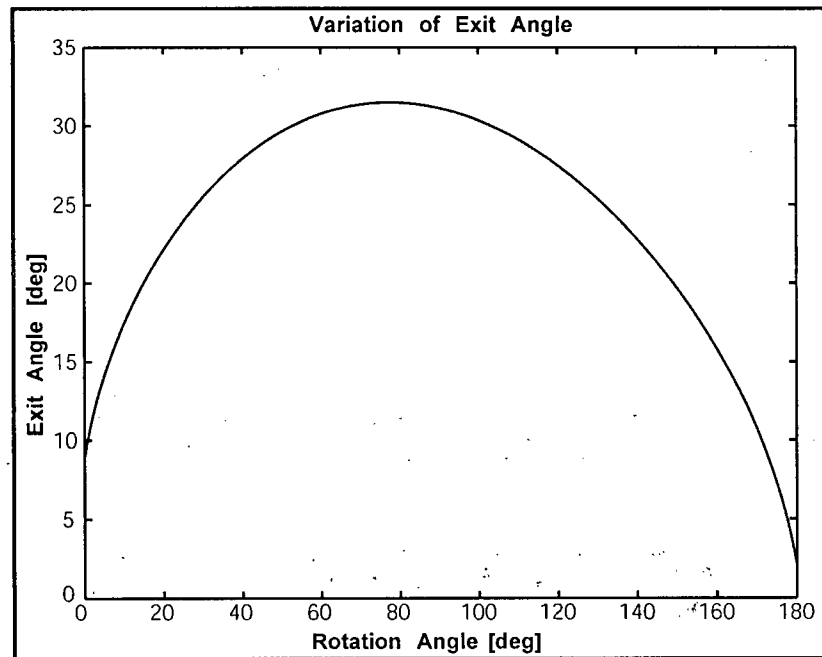


Figure 3.8 : Variation of exit angle during the rotation of the tool around the workpiece

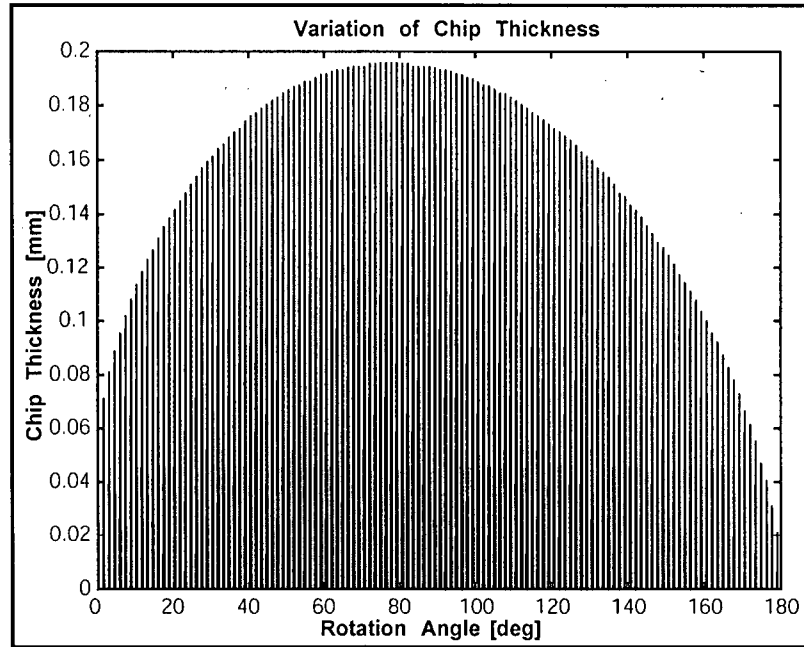


Figure 3.9 : Variation of chip thickness during the rotation of the tool around the workpiece

Chapter 4

Direct Method for Chatter Stability of Milling Operation

4.1. Introduction

Rotating cutting forces that continuously change direction of oscillation are generated during milling operation. As periodic cutting forces excite one of the structural modes of the machine tool-workpiece structure, the cutting tool begins to vibrate and the flute in cut leaves a wavy surface on the workpiece. Each flute removes the existing surface and continue to leave a wavy surface behind (See Figure 4.1), creating chips with waves on both sides. If two waves are in phase, dynamic chip thickness stays constant during milling operation and forced vibrations occur in the machine tool-workpiece structure. If there is a phase shift between these two waves, the dynamic chip thickness and the periodic dynamic cutting forces may increase exponentially, and the machine tool-workpiece structure experiences self excited vibrations called chatter. Chatter vibrations are dependent on the previous tooth pass, hence the mathematical representation of dynamics of milling operation contains a time delay term.

A new analytical method, called Direct method, was developed for the stability of linear time invariant time delay systems by Sipahi et al. [31]. The difficulty in investigating the stability of time delay systems is that they have infinite number of roots, and up to now there have been no methods reported to find exact solution.

Direct method is an exact and a general solution to stability of time delay systems, and it can be applied to milling process for assessment of stability lobes. In this chapter, Direct method is introduced, then steps followed for implementation to single degree of freedom (SDOF) milling operation are described. The stability lobes constructed from Direct method are compared to the stability lobes simulated by using frequency domain solution developed by Altintas et al. [12] and experimental results presented by Bayly et al. [8].

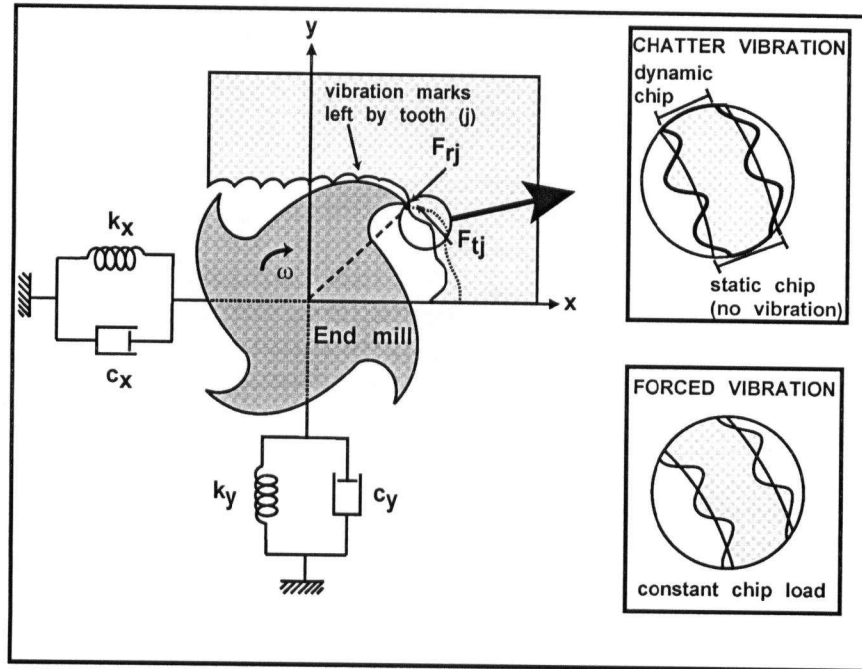


Figure 4.1 : Regenerative effect in milling operation

4.2. Direct Method

A general time delay expression [31] in state space form given by following equation:

$$\dot{x}(t) = [A]x(t) + [B]x(t - \tau) + [G]\dot{x}(t - \tau) \quad (4.1)$$

where;

$x(n \times 1)$ state vector,

$[A]_{n \times n}$, $[B]_{n \times n}$, $[G]_{n \times n}$ constant state matrices,

$[B]_{n \times n}$ state feedback matrix,

$[G]_{n \times n}$ derivative part of control,

τ time delay ($\tau \geq 0$ for causality reasons)

Dynamic behavior of a time delay system is investigated by calculating roots of characteristic equation. By taking Laplace transformation of Equation (4.1) the time delay expression can be represented in s -domain:

$$sx(s) = [A]x(s) + [B]e^{-\tau s}x(s) + [G]se^{-\tau s}x(s) \quad (4.2)$$

$$(sI - [A] - [B]e^{-\tau s} - [G]se^{-\tau s})x(s) = 0 \quad (4.3)$$

The characteristic equation of the time delay system is the determinant of Equation (4.3).

$$CE(s, \tau) = \det(sI - [A] - [B]e^{-\tau s} - [G]se^{-\tau s}) = 0 \quad (4.4)$$

Three different states are used to describe the dynamics of a system i.e. stable, unstable and critically stable state. Critically stable conditions form a boundary between stable and unstable conditions. The main goal is to identify time delay values τ at which the dynamic system is critically stable. D Subdivision method [19] is used in Direct method. According to D Subdivision method, there are regions, so-called pockets, in which the number of stable and unstable roots are fixed. Therefore the characteristic equation of the time delay system given by Equation (4.4) has at least one pair of purely imaginary roots $s = \pm\omega_r i$ while crossing the boundaries between these regions. ω_r defines frequency in [Hz]. The time delay values τ corresponding to the purely imaginary roots $s = \pm\omega_r i$ represent transition from a stable state to an unstable state or vice versa. Equation (4.4) has infinite number of roots because of the time delay term $e^{-\tau s}$. Therefore in order to simplify solution of the characteristic equation (Equation (4.4)) time delay term $e^{-\tau s}$ can be replaced with a bilinear expression [29] shown below:

$$e^{-\tau s} = \frac{1 - Ts}{1 + Ts} \quad (4.5)$$

The equality given by Equation (4.5) is exact and valid only when the time delay system is in critically stable state (the time delay system has purely imaginary roots $s = \pm\omega_r i$). The relation between the time delay τ (positive real number) and T (real number) is written as:

$$e^{-i\omega_r\tau} = \cos \omega_r\tau - i \sin \omega_r\tau = \frac{1 - i\omega_r T}{1 + i\omega_r T} \quad (4.6)$$

$$\cos \omega_r\tau = \frac{1 - (\omega_r T)^2}{1 + (\omega_r T)^2}, \quad \sin \omega_r\tau = \frac{2\omega_r T}{1 + (\omega_r T)^2} \quad (4.7)$$

$$\tan \frac{\omega_r\tau}{2} = \frac{\sin \omega_r\tau}{1 + \cos \omega_r\tau} = \left(\frac{2\omega_r T}{1 + (\omega_r T)^2} \right) \left(\frac{1}{1 + \frac{1 - (\omega_r T)^2}{1 + (\omega_r T)^2}} \right) = \omega_r T = \omega_r T + l\pi \quad (4.8)$$

$$\tau = \frac{2}{\omega_r} [\text{atan}(\omega_r T) + l\pi] \quad (4.9)$$

where $l = l_0, l_0 + 1, l_0 + 2, l_0 + 3; \dots \infty$, l_0 is the smallest positive integer number that makes the time delay τ given by Equation (4.9) greater than zero. After substitution of bilinear expression (Equation (4.5)) into the characteristic equation given by Equation (4.4), resultant characteristic equation which has n number of roots is obtained as a function of s and T :

$$CE(s, T) = \det \left(sI - [A] - [B] \left(\frac{1 - Ts}{1 + Ts} \right) - [G] s \left(\frac{1 - Ts}{1 + Ts} \right) \right) = 0 \quad (4.10)$$

$$CE = \det \left(\begin{bmatrix} s & \dots & 0 \\ \dots & \dots & \dots \\ 0 & \dots & s \end{bmatrix} - \begin{bmatrix} A_{11} & \dots & A_{1n} \\ \dots & \dots & \dots \\ A_{n1} & \dots & A_{nn} \end{bmatrix} - \left(\frac{1 - Ts}{1 + Ts} \right) \left(\begin{bmatrix} B_{11} & \dots & B_{1n} \\ \dots & \dots & \dots \\ B_{n1} & \dots & B_{nn} \end{bmatrix} - s \begin{bmatrix} G_{11} & \dots & G_{1n} \\ \dots & \dots & \dots \\ G_{n1} & \dots & G_{nn} \end{bmatrix} \right) \right) = 0$$

$$CE(s, T) = \det \begin{pmatrix} s - A_{11} - \left(\frac{1-Ts}{1+Ts}\right)(B_{11} - sG_{11}) & \dots & -A_{1n} - \left(\frac{1-Ts}{1+Ts}\right)(B_{1n} - sG_{1n}) \\ \dots & \dots & \dots \\ -A_{n1} - \left(\frac{1-Ts}{1+Ts}\right)(B_{n1} - sG_{n1}) & \dots & s - A_{nn} - \left(\frac{1-Ts}{1+Ts}\right)(B_{nn} - sG_{nn}) \end{pmatrix} = 0$$

$$CE(s, T) = \left(\frac{1}{(1+Ts)^n} \sum_{r=0}^{2n} m_r s^{2n-r} \right) + \sum_{r=0}^n b_r s^{n-r} = 0 \quad (4.11)$$

where $m_r = m_r(T)$ and b_r is an integer. Equation (4.11) is multiplied by $(1+Ts)^n$ to eliminate the denominator, hence new characteristic equation becomes $(2n)^{th}$ order polynomial:

$$CE_{new}(s, T) = \sum_{k=0}^{2n} a_r s^{2n-r} = 0 \quad (4.12)$$

where $a_r = a_r(T)$. Although order of the characteristic equation of the time delay system (Equation (4.11)) increases, both equations (Equation (4.11) and Equation (4.12)) have the same imaginary axis crossings, furthermore Equation (4.12) is easier to solve.

By using the coefficients of the characteristic equation given by Equation (4.12), elements of Routh-Hurwitz array [20] are formed to find the purely imaginary roots. The idea behind Routh-Hurwitz is to find number of unstable roots without solving the characteristic equation of time delay system. The information about stability of the time delay system can be obtained by using only the coefficients of the characteristic equation (Equation (4.12)). The new characteristic equation of the time delay system (Equation (4.12)) can be extended as follows:

$$a_0 s^{2n} + a_1 s^{2n-1} + a_2 s^{2n-2} + \dots + a_{2n-1} s + a_{2n} = 0 \quad (4.13)$$

Since the order of the characteristic equation of the time delay system (Equation (4.13)) is $2n$, Routh-Hurwitz array becomes $(2n + 1) \times (2n + 1)$ matrix. The general representation for Routh-Hurwitz array and calculation of the elements are as follows:

$$\begin{bmatrix}
 a_0 & a_2 & a_4 & \dots & a_{2n} & \dots & 0 & \dots & 0 \\
 a_1 & a_3 & a_5 & \dots & a_{2n-1} & \dots & 0 & \dots & 0 \\
 b_1 & b_2 & b_3 & \dots & \dots & \dots & 0 & \dots & 0 \\
 \dots & \dots & \dots & \dots & \dots & \dots & 0 & \dots & 0 \\
 h_1 & h_2 & h_3 & \dots & \dots & \dots & 0 & \dots & 0 \\
 \dots & \dots & \dots & \dots & \dots & \dots & 0 & \dots & 0 \\
 u_1 & u_2 & u_2 & \dots & \dots & \dots & 0 & \dots & 0 \\
 \dots & \dots & \dots & \dots & \dots & \dots & 0 & \dots & 0
 \end{bmatrix}_{(2n+1) \times (2n+1)} \quad (4.14)$$

Sample calculations for some of the elements of Routh-Hurwitz array are given by following expressions [20]:

$$\begin{aligned}
 b_1 &= \frac{a_1 a_2 - a_0 a_3}{a_1} \\
 b_2 &= \frac{a_1 a_4 - a_0 a_5}{a_1} \\
 &\dots \\
 c_1 &= \frac{b_1 a_3 - a_1 b_2}{b_1} \\
 c_2 &= \frac{b_1 a_5 - a_1 b_3}{b_1} \\
 &\dots \\
 d_1 &= \frac{c_1 b_2 - c_2 b_1}{c_1} \\
 &\dots \\
 u_1 &= \frac{t_1 s_2 - t_2 s_1}{t_1}
 \end{aligned} \tag{4.15}$$

The number of sign changes (NS) in the first column of the Routh-Hurwitz array in Equation (4.14) gives the number of unstable roots of the characteristic equation (NU) expressed by Equation (4.13). Routh-Hurwitz array of a second order system is given as an example:

$$\begin{array}{l}
 \left[\begin{array}{l}
 \text{Positive } a_2 \ a_4 \ 0 \ 0 \\
 \text{Negative } a_3 \ 0 \ 0 \ 0 \\
 \text{Negative } b_2 \ 0 \ 0 \ 0 \\
 \text{Positive } 0 \ 0 \ 0 \ 0 \\
 \text{Positive } 0 \ 0 \ 0 \ 0
 \end{array} \right]_{5 \times 5} \rightarrow n = 2 \rightarrow NS = NU = 2
 \end{array}$$

There are two special cases that have to be taken into account when using Routh-Hurwitz array [20]. Some difficulties occur in the calculation of number of sign changes in the first column of Routh-Hurwitz array when only the first element of any one row is zero and the rest of the elements are nonzero, or all the elements of one row are zero. To solve the first problem, zero in the first column of the row is replaced by a small positive integer number ν or the characteristic equation of the system is multiplied by $s + d$ where d is an arbitrary positive number. In the sec-

ond case, the zero row is handled by taking derivative of the equation formed by using the elements of the row above the zero row, then the elements of zero row is replaced by the coefficients of the new equation.

The elements in the first column of Routh-Hurwitz array given by Equation (4.14) are a function of T . By scanning T from $-\infty$ to ∞ various Routh-Hurwitz arrays are obtained representing the time delay system. The number of sign changes in the first column may change between subsequent T values. When the number of sign changes is different from the previous one, an imaginary axis crossing is assumed to occur. The characteristic equation given by Equation (4.13) has two purely conjugate imaginary roots if the difference in number of sign changes between subsequent T values equals 2. If the difference is 1, one of the roots is equal to 0. The difference ($NS_{previous} - NS_{current}$) can be either positive or negative. If the difference is positive, the dynamic time delay system may change its state from unstable to stable as following:

$$\begin{array}{l}
 \left[\begin{array}{l}
 \text{Positive } a_2 \ a_4 \ 0 \ 0 \\
 \text{Negative } a_3 \ 0 \ 0 \ 0 \\
 \text{Negative } b_2 \ 0 \ 0 \ 0 \\
 \text{Positive } 0 \ 0 \ 0 \ 0 \\
 \text{Positive } 0 \ 0 \ 0 \ 0
 \end{array} \right]_{5 \times 5} \rightarrow NS = NU = 2 \rightarrow T_{previous} \\
 \\
 \left[\begin{array}{l}
 \text{Positive } a_2 \ a_4 \ 0 \ 0 \\
 \text{Positive } a_3 \ 0 \ 0 \ 0 \\
 \text{Positive } b_2 \ 0 \ 0 \ 0 \\
 \text{Positive } 0 \ 0 \ 0 \ 0 \\
 \text{Positive } 0 \ 0 \ 0 \ 0
 \end{array} \right]_{5 \times 5} \rightarrow NS = NU = 0 \rightarrow T_{present}
 \end{array} \quad (4.16)$$

The purely imaginary roots of the characteristic equation (Equation (4.13)) is evaluated based on present T . If T is a negative real number, multiplication of a second order characteristic equation ($n = 2$ in Equation (4.11)) by $(1 + Ts)^2$ brings 2 unstable roots to the time delay system. In order to decide whether the state of dynamic system is stable or not, unstable roots coming from

negative T have to be considered during investigation of the stability. The second order system is stable if:

$$NS = NU = 0 \quad \text{and} \quad T > 0$$

$$NS = NU = 2 \quad \text{and} \quad T < 0$$

The time delay τ is found by substituting the obtained purely imaginary root ω_r and present T values in Equation (4.9). Investigation of stability of a time delay system is concluded by calculating the time delay τ .

4.3. Stability of a Single Degree of Freedom Milling Operation

Dynamics of a single degree of freedom (SDOF) milling system and application of Direct method to investigate stability of the system are explained in the section.

Since milling operation is an intermittent cutting operation and the periodic cutting forces change direction of oscillation, dynamics of milling operation is very complicated. In general, at least two orthogonal degrees of freedom need to be taken into account. Depending on the machine tool-workpiece structure, milling system can be simplified to a single degree of freedom system. If modal parameters of machine-tool-workpiece structure in one direction are significantly higher than modal parameters in other directions, the system is rigid in all other directions and therefore considered to be a SDOF system. The system can also be assumed a SDOF system if the radial width of cut is small (low immersion angle).

A SDOF milling system shown in Figure 4.2 consists of mass m_x , dash pot c_x and spring k_x elements. The tool rotates with a spindle speed of ω [rad/sec], and the workpiece is fed towards the tool with a feed rate of s_t [mm/rev/tooth]. Immersion angle ($\phi = \phi(t) = \omega t$) is measured from positive y axis in clockwise direction, and radial width of cut is defined by entry ϕ_{st} and exit ϕ_{ex} angles. The periodic cutting forces generated in tangential $F_{tj}(t)$ and radial $F_{rj}(t)$ directions at tool-workpiece contact point are calculated as follows:

$$\begin{aligned} F_{tj}(t) &= K_{tc} b h_j(t) \\ F_{rj}(t) &= K_{rc} b h_j(t) \end{aligned} \quad (4.17)$$

j represents the flute number K_{tc} and K_{rc} are empirical cutting force coefficients in tangential and radial directions, b is axial depth of cut, h is dynamic chip thickness $\phi_j = \phi + (j-1)\phi_p$ is instantaneous angular immersion of flute j and ϕ_p is the pitch angle of the milling cutter.

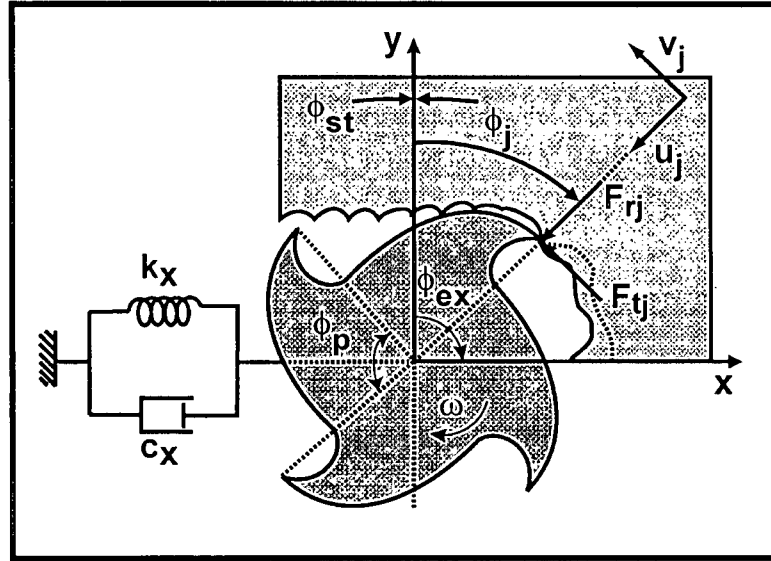


Figure 4.2 : A single degree of freedom milling system

Dynamic chip thickness $h_j(t)$ is expressed in terms of feed rate (s_t), instantaneous angular immersion (ϕ_j) of j^{th} flute, dynamic displacement of tool in chip thickness direction at current ($u(t) = u_j$) and at previous ($u(t-\tau) = u_{j-1}$) passes:

$$h_j(t) = s_t \sin \phi_j + \{u(t-\tau) - u(t)\} \quad (4.18)$$

Dynamic displacements in chip thickness direction $\{u(t), u(t-\tau)\}$ can be expressed as a function of structural vibrations in x direction:

$$\{u(t-\tau) - u(t)\} = \{x(t) - x(t-\tau)\} \sin \phi_j \quad (4.19)$$

Time delay τ is equal to the tooth passing period $\frac{2\pi}{N\omega}$ in milling operation. Equation of motion of the milling system can be described by projecting the periodic cutting forces in tangential $F_{tj}(t)$

and radial $F_{rj}(t)$ directions given by Equation (4.17) on x axis. The total periodic cutting force in x direction is obtained by summing forces generated by all flutes which are in cut:

$$F_x(t) = \sum_{j=1}^N g(\phi_j) [-F_{tj}(t) \cos \phi_j - F_{rj}(t) \sin \phi_j] \quad (4.20)$$

To determine whether the j^{th} flute is in cut or out of cut a step function $g(\phi_j)$ is used:

$$\begin{aligned} \phi_{st} \leq \phi_j \leq \phi_{ex} &\rightarrow g(\phi_j) = 1 \\ \phi_j < \phi_{st} \quad \phi_{ex} < \phi_j &\rightarrow g(\phi_j) = 0 \end{aligned} \quad (4.21)$$

When the periodic cutting forces ($F_x(t)$) expressed in Equation (4.20) excite the machine tool-workpiece structure, the equation of motion for the milling system can be represented by:

$$m_x \ddot{x}(t) + c_x \dot{x}(t) + k_x x(t) = F_x(t) \quad (4.22)$$

By substituting Equations (4.17), (4.18) and (4.20) into Equation (4.22):

$$m_x \ddot{x}(t) + c_x \dot{x}(t) + k_x x(t) = \frac{1}{2} K_{tc} b a_x(t) \{x(t) - x(t - \tau)\} \quad (4.23)$$

where

$$a_x(t) = \sum_{j=1}^N -g(\phi_j) [\sin 2\phi_j + K_r (1 - \cos 2\phi_j)] \quad (4.24)$$

$K_r = \frac{K_{rc}}{K_{tc}}$ is the ratio between radial (K_{rc}) and tangential (K_{tc}) cutting coefficients and $a_x(t)$ is time varying directional milling coefficient, which is periodic at tooth passing period. By consid-

ering only zero order term of its Fourier series expansion, the time variation of the directional coefficient is eliminated:

$$a_{x0} = \frac{1}{\tau} \int_0^{\tau} a_x(t) dt \quad (4.25)$$

a_{x0} can be written as a function of instantaneous immersion angle ϕ by substituting t by ϕ into Equation (4.25):

$$\alpha_{x0} = \frac{1}{\phi_p - \phi_{st}} \int_{\phi_{st}}^{\phi_{ex}} a_x(\phi) d\phi \quad (4.26)$$

Resultant average directional milling coefficient α_{x0} becomes:

$$\alpha_{x0} = \frac{N}{2\pi} \left(\frac{1}{2} [\cos 2\phi - 2K_r \phi - K_r \sin 2\phi] \right) \Bigg|_{\phi_{st}}^{\phi_{ex}} \quad (4.27)$$

By substituting Equation (4.27) into Equation (4.23), the regenerative milling system dynamics is reduced to the following delayed differential equation:

$$m_x \ddot{x}(t) + c_x \dot{x}(t) + k_x x(t) = \frac{1}{2} K_{tc} b \alpha_{x0} \{x(t) - x(t - \tau)\} \quad (4.28)$$

Direct method of Sipahi et al. [31] is applied to the milling system with flexibility in x direction. The structural displacement and velocity of the vibrating system are considered as states:

$$\begin{aligned}
 x_1(t) &= x(t) \\
 x_2(t) &= \dot{x}_1(t) = \dot{x}(t) \\
 \dot{x}_2(t) &= \ddot{x}_1(t) = \ddot{x}(t)
 \end{aligned} \tag{4.29}$$

State space representation of the SDOF milling system is formed by substituting the states into Equation (4.28):

$$\begin{bmatrix} 1 & 0 \\ 0 & m_x \end{bmatrix} \begin{bmatrix} \dot{x}_1(t) \\ \dot{x}_2(t) \end{bmatrix} = \begin{bmatrix} 0 & 1 \\ -k_x + \frac{1}{2}K_{tc}b\alpha_{x0} & -c_x \end{bmatrix} \begin{bmatrix} x_1(t) \\ x_2(t) \end{bmatrix} - \begin{bmatrix} 0 & 0 \\ \frac{1}{2}K_{tc}b\alpha_{x0} & 0 \end{bmatrix} \begin{bmatrix} x_1(t-\tau) \\ x_2(t-\tau) \end{bmatrix} \tag{4.30}$$

In order to express the equation of motion in the form of $\dot{x}(t) = Ax(t) + Bx(t-\tau) + G\dot{x}(t-\tau)$ (Equation (4.1)), Equation (4.30) is multiplied by the inverse of $\begin{bmatrix} 1 & 0 \\ 0 & m_x \end{bmatrix}$:

$$\begin{bmatrix} \dot{x}_1(t) \\ \dot{x}_2(t) \end{bmatrix} = \begin{bmatrix} 1 & 0 \\ 0 & m_x \end{bmatrix}^{-1} \begin{bmatrix} 0 & 1 \\ -k_x + \frac{1}{2}K_{tc}b\alpha_{x0} & -c_x \end{bmatrix} \begin{bmatrix} x_1(t) \\ x_2(t) \end{bmatrix} - \begin{bmatrix} 1 & 0 \\ 0 & m_x \end{bmatrix}^{-1} \begin{bmatrix} 0 & 0 \\ \frac{1}{2}K_{tc}b\alpha_{x0} & 0 \end{bmatrix} \begin{bmatrix} x_1(t-\tau) \\ x_2(t-\tau) \end{bmatrix} \tag{4.31}$$

where

$$[A]_{2 \times 2} = \begin{bmatrix} 0 & 1 \\ \frac{1}{m_x} \left(-k_x + \frac{1}{2}K_{tc}b\alpha_{x0} \right) & \frac{1}{m_x} (-c_x) \end{bmatrix}_{2 \times 2}$$

$$[B]_{2 \times 2} = \begin{bmatrix} 0 & 0 \\ \frac{1}{m_x} \left(-\frac{1}{2}K_{tc}b\alpha_{x0} \right) & 0 \end{bmatrix}_{2 \times 2}$$

$$[G]_{2 \times 2} = \begin{bmatrix} 0 & 0 \\ 0 & 0 \end{bmatrix}_{2 \times 2}$$

Since $[G]$ is a zero matrix, the milling system is called a retarded time delay system and therefore characteristic equation of SDOF milling system can be found by substituting only $[A]$ and $[B]$ matrices into Equation (4.10):

$$CE(s, T) = \det \left[sI - [A]_{2 \times 2} - \left(\frac{1 - Ts}{1 + Ts} \right) [B]_{2 \times 2} \right] = 0$$

$$CE(s, T) = \det \left[sI - \begin{bmatrix} 0 & 1 \\ \left(\frac{-k_x + \frac{1}{2}K_{tc}b\alpha_x}{m_x} \right) & \left(\frac{-c_x}{m_x} \right) \end{bmatrix}_{2 \times 2} - \left(\frac{1 - Ts}{1 + Ts} \right) \begin{bmatrix} 0 & 0 \\ \left(\frac{-\frac{1}{2}K_{tc}b\alpha_x}{m_x} \right) & 0 \end{bmatrix}_{2 \times 2} \right] = 0 \quad (4.32)$$

To simplify the solution of the characteristic equation, Equation (4.32) is multiplied with $(1 + Ts)^2$, and the new $(2n)^{th} = 4^{th}$ order characteristic equation with a form similar to Equation (4.13):

$$a_0 s^4 + a_1 s^3 + a_2 s^2 + a_3 s + a_4 = 0$$

$$a_0 = T^2$$

$$a_1 = \frac{c_x T^2}{m_x} + 2T$$

$$a_2 = \frac{k_x T^2 + 2c_x T - K_{tc} b \alpha_{x0} T^2}{m_x} + 1$$

$$a_3 = \frac{2k_x T + c_x - K_{tc} b \alpha_{x0} T}{m_x}$$

$$a_4 = \frac{k_x}{m_x}$$
(4.33)

By using the polynomial coefficients a_0, a_1, a_2, a_3, a_4 given by Equations (4.33) and (4.15), the elements of Routh-Hurwitz array are evaluated:

$$\begin{bmatrix} a_0 & a_2 & a_4 & 0 & 0 \\ a_1 & a_3 & 0 & 0 & 0 \\ b_1 & b_2 & 0 & 0 & 0 \\ c_1 & 0 & 0 & 0 & 0 \\ d_1 & 0 & 0 & 0 & 0 \end{bmatrix} \quad (4.34)$$

The elements of Routh-Hurwitz array given by Equation (4.34) are functions of (T) and axial depth of cut b . By scanning T from $-\infty$ to ∞ for a desired axial depth of cut b , Routh-Hurwitz arrays are evaluated and the number of sign changes in the first column of each array is detected. For the corresponding T values, where the number of sign changes varies, the characteristic equation of the SDOF milling system given by Equation (4.33) is solved based on the present value of T to find purely imaginary roots $s = \pm\omega_r i$. Minimum positive integer l_0 which makes the tooth passing period τ greater than zero is found by substituting present value of T and corresponding positive value of ω_r into Equation (4.9), and by incrementing the l_0 by one, tooth passing period values of τ are evaluated. Spindle speed (n), where the milling system behaves critically stable for the given axial depth of cut b , can be obtained as:

$$n = \frac{60}{N\tau} \quad (4.35)$$

The stability lobes of the SDOF milling system can be evaluated by repeating the given steps for the specified range of axial depth of cut b .

4.4. Simulations

A MATLAB program has been developed to evaluate the validity and applicability of the method applied to the milling stability problem. The stability lobes are simulated by using both the Direct method and the frequency domain solution proposed by Altintas et al. [12] and compared against each other.

In the simulations, a cylindrical end mill having $R_c = 9.525$ [mm] radius with 2 flutes is used for slotting operation. Al 7050T6 is selected as workpiece. The dynamic parameters of the SDOF milling system in x direction are natural frequency $\omega_{nx} = 500$ [Hz], stiffness $k_x = 10^4$ [N/mm] and damping ratio $\xi_x = 0.05$. Since the stiffness values in y and z directions are assumed to be 10 times greater than the stiffness value in x direction, the milling system is considered as rigid in y and z directions. The cutting coefficients in tangential and radial directions are $K_{tc} = 900$ [N/mm²], $K_{rc} = 270$ [N/mm²]. Axial depth of cut b is scanned from 3 [mm] to 25 [mm] and T is swept from -6×10^{-2} to -1×10^{-7} . The step sizes for axial depth of cut b and T are $\Delta b = 2$ [mm] and $\Delta T = 1 \times 10^{-7}$. The purely imaginary root of the characteristic equation $s = \omega_c i$ show chatter frequency ω_c for given axial depth of cut b and tooth period τ .

The simulated stability lobes are shown in Figure 4.3, where frequency domain solution and direct method are in consistent. Also, if point A ($b = 4.99742$ [mm], $n = 5000$ [rpm]) in Figure 4.3 is considered, both methods give the same chatter frequency $\omega_c = 550.6$ [Hz] as well.

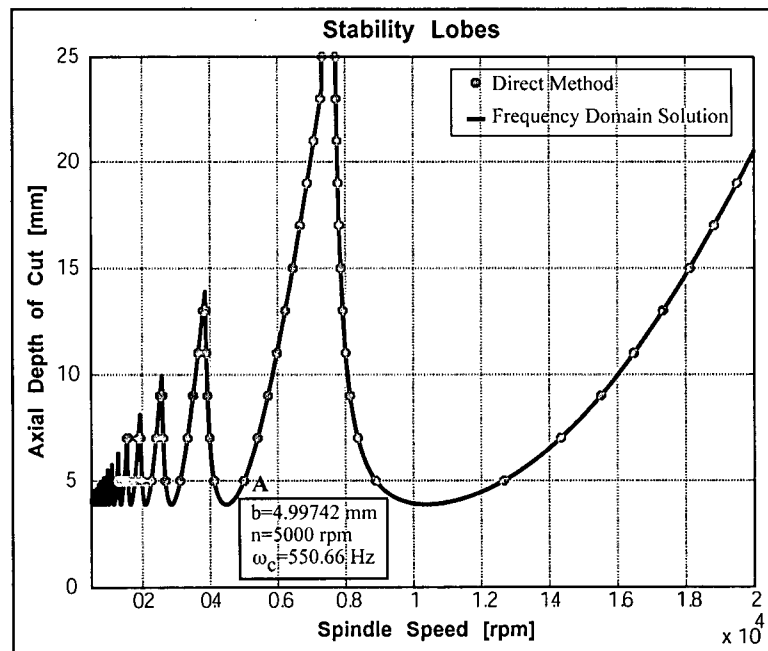


Figure 4.3 : Comparison of direct method with frequency domain solution

Stability lobes are also constructed for different cutting conditions in order to compare the Direct method with experimental results published by Bayly et al. [8]. In the experiments, a cylindrical end mill having $R_c = 9.525$ [mm] radius with one flute was used. Modal parameters in x direction were natural frequency $\omega_{nx} = 146.5$ [Hz], stiffness $k_x = 2.18 \times 10^3$ [N/mm] and damping ratio $\xi_x = 0.0032$. Setup of the experiment was designed in such a way that stiffness values in y and z directions are more than 20 times greater than the stiffness value in x direction. The cutting coefficients in tangential and radial directions were $K_{tc} = 550$ [N/mm²], $K_{rc} = 200$ [N/mm²] respectively. The ratio between time in cut t_c and total time was $\rho = 0.162$.

In the simulation, scanning range for axial depth of cut b is from 0.3 [mm] to 3.9 [mm] and for T is from -3×10^{-1} to -1×10^{-4} . The step sizes for axial depth of cut b and T are $\Delta b = 0.3$ [mm] and $\Delta T = 5 \times 10^{-5}$. The simulated stability lobes and experimental results are shown in Figure 4.4. They are in good agreement.

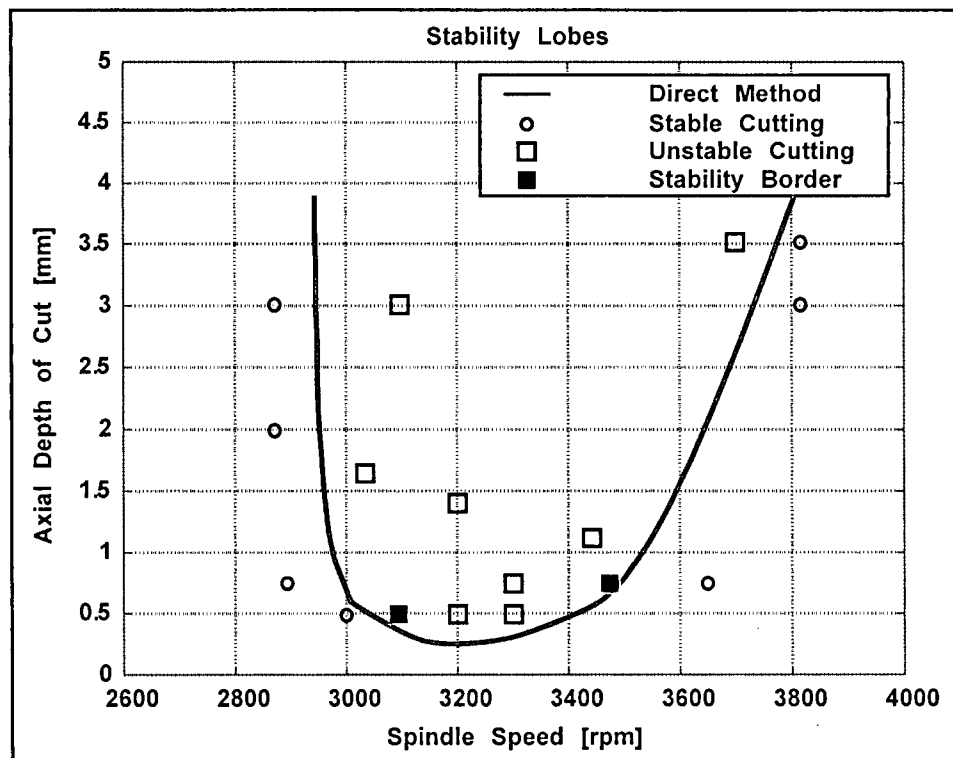


Figure 4.4 : Comparison of direct method with experiments

The disadvantage of the Direct method is its long computational time. The MATLAB program for Direct method takes approximately 1 day. The most time consuming part of Direct method is scanning of T values with very small increments between $-\infty$ to ∞ for each axial depth of cut b value. Later, Sipahi & Olgac improved their method by including a new algorithm and the computational time for new method (CTRC method) is same as the frequency domain solution.

Chapter 5

Dynamics of Circular Milling Operation

5.1. Introduction

Chatter is a self excited vibration originated by regenerative effect caused by phase shift between two successive waves left on both sides of the chip during circular milling operation. Since the poor surface finish, tool breakage, tool wear and large dynamic loads on machine tool structure are the main outcomes of chatter, dynamics of the circular milling operation has to be investigated in order to increase the quality of the process and material removal rate. Dynamics of regular milling operation has been summarized in Chapters 2 and 4. Dynamics of circular milling operations is more complicated than regular milling operations due to the planetary motion of the tool around the workpiece. Cutting forces are periodic not only at tooth passing period but also at period of circular motion of the tool around the workpiece. Although variation in entry ϕ_{st} and exit ϕ_{ex} angles of the tool brings additional complexity to the dynamics, varying radial depth of cut may cause a shift in stability lobes. In this chapter, dynamic cutting forces are discussed and two analytical approaches, namely frequency domain solution presented by Altintas et al. [4] and time finite element method developed by Bayly et al. [8], are used to investigate the chatter stability of circular milling. Finally the theoretical stability lobes are compared with the experimental results.

5.2. Dynamics of Circular Milling

Dynamic cutting forces excite the machine tool-workpiece structure in global x and y directions and form dynamic displacements. Dynamic displacement in chip thickness direction is evaluated in terms of tool's angular position, θ , instantaneous immersion angle ϕ_j of tooth j , and vibrations in global coordinates as follows:

$$h(\theta, \phi_j) = s_t \sin(\phi_j) + \Delta x \sin(\theta + \phi_j) + \Delta y \cos(\theta + \phi_j) \quad (5.1)$$

where

$$h(\phi_j) = s_t \sin \phi_j + \Delta x_c(t) \sin \phi_j + \Delta y_c(t) \cos \phi_j$$

$$\Delta x_c(t) = \Delta x(t) \cos \theta - \Delta y(t) \sin \theta$$

$$\Delta y_c(t) = \Delta x(t) \sin \theta + \Delta y(t) \cos \theta$$

$s_t \sin(\phi_j)$ defines the static part and $\Delta x(t) \sin(\theta + \phi_j) + \Delta y(t) \cos(\theta + \phi_j)$ represents the dynamic part of chip thickness in Equation (5.1). $h(\phi_j)$ is the dynamic chip thickness in tool coordinates, x_c and y_c . $\Delta x_c(t) = x_c(t) - x_c(t - \tau)$ and $\Delta y_c(t) = y_c(t) - y_c(t - \tau)$ express difference between dynamic displacements at previous and current cuts in x_c and y_c directions. $\Delta x(t) = x(t) - x(t - \tau)$ and $\Delta y(t) = y(t) - y(t - \tau)$ show the same difference in global coordinates. Since the static part has no effect on stability [3], $s_t \sin(\phi_j)$ can be eliminated from the chip thickness definition in Equation (5.1) and the resultant dynamic chip thickness expression becomes:

$$h(\theta, \phi_j) = \Delta x(t) \sin(\theta + \phi_j) + \Delta y(t) \cos(\theta + \phi_j) \quad (5.2)$$

Dynamic cutting forces acting on tooth j in global coordinates F_{xj}, F_{yj} can be evaluated as a function of cutting coefficients K_{tc}, K_r , axial depth of cut b , chip thickness h , angular position of the tool θ and instantaneous immersion angle of tooth j ϕ_j as follows:

$$\begin{aligned} F_x(\theta, \phi_j) &= -K_{tc} b h(\theta, \phi_j) [\cos(\theta + \phi_j) + K_r \sin(\theta + \phi_j)] \\ F_y(\theta, \phi_j) &= -K_{tc} b h(\theta, \phi_j) [-\sin(\theta + \phi_j) + K_r \cos(\theta + \phi_j)] \end{aligned} \quad (5.3)$$

By substituting Equation (5.2) into Equation (5.3):

$$\begin{Bmatrix} F_{xj} \\ F_{yj} \end{Bmatrix} = \frac{1}{2} K_{tc} b \begin{bmatrix} -K_r - \sin 2E + K_r \cos 2E & -1 - K_r \sin 2E - \cos 2E \\ 1 - \cos 2E - K_r \sin 2E & -K_r - K_r \cos 2E + \sin 2E \end{bmatrix} \begin{Bmatrix} \Delta x(t) \\ \Delta y(t) \end{Bmatrix} \quad (5.4)$$

where

$$E = \theta + \phi_j \quad (5.5)$$

Total dynamic cutting forces F_x, F_y are calculated by summing the forces generated by each tooth j F_{xj}, F_{yj} in Equation (5.4):

$$\begin{aligned} F_x(\theta, \phi) &= \sum_{j=1}^N F_{xj} \\ F_y(\theta, \phi) &= \sum_{j=1}^N F_{yj} \end{aligned} \quad (5.6)$$

$$\{F(t)\} = \frac{1}{2} K_{tc} b [D(t)] \{\Delta(t)\} \quad (5.7)$$

where

$$[D(t)] = \begin{bmatrix} d_{xx} & d_{xy} \\ d_{yx} & d_{yy} \end{bmatrix} \text{ is directional milling coefficient matrix and}$$

$d_{xx}, d_{xy}, d_{yx}, d_{yy}$ are directional milling coefficients in global coordinates which show the direction of excitation as the tool rotates during circular milling operation given by:

$$\begin{aligned}
d_{xx}(\theta, \phi) &= \sum_{j=1}^N g_j(\phi_j) [-K_r - \sin 2E + K_r \cos 2E] \\
d_{xy}(\theta, \phi) &= \sum_{j=1}^N g_j(\phi_j) [-1 - K_r \sin 2E - \cos 2E] \\
d_{yx}(\theta, \phi) &= \sum_{j=1}^N g_j(\phi_j) [1 - \cos 2E - K_r \sin 2E] \\
d_{yy}(\theta, \phi) &= \sum_{j=1}^N g_j(\phi_j) [-K_r - K_r \cos 2E + \sin 2E]
\end{aligned} \tag{5.8}$$

5.3. Analytical Chatter Stability

In this section, two analytical models, namely frequency domain solution developed by Altintas et al. [12] and time finite element analysis proposed by Bayly et al. [8] are applied to the stability of circular milling process.

5.3.1. Frequency Domain Solution

The frequency domain solution introduced by Altintas et al. [12] is a practical method for the assessment of stability of milling operations that defines the dynamics in terms of material properties, tool-workpiece intersections, tool geometry and frequency response function of machine tool structure [4]. The analytical model is based on linear system, and the circular milling dynamics need to be simplified based on the physics of the process.

Directional milling coefficients are periodic at tooth passing period τ as well as at period of the tool's planetary motion around the workpiece ($T_p = \frac{60}{n_p} = \frac{2\pi}{\Omega}$). Since the problem is very complicated from mathematical point of view due to presence of double periodicity, the directional matrix is expanded for the tooth passing period τ :

$$[D(t)] = \sum_{r=-\infty}^{\infty} [D_r] e^{ir\omega_\tau t} \quad (5.9)$$

$$[D_r] = \frac{1}{\tau} \int_0^\tau [D(t)] e^{-ir\omega_\tau t} dt$$

In order to simplify the solution only the zero order term of Fourier series is considered:

$$[D_0] = \frac{1}{\tau} \int_0^\tau [D(t)] dt \quad (5.10)$$

Angular position of the tool around the workpiece θ and time t are written in terms of instantaneous immersion angle ϕ to decrease the number of unknown variables in Equation (5.10):

$$\theta = \Omega t, \quad \phi = \omega t \rightarrow \theta = \frac{\Omega}{\omega} \phi = \frac{1}{H} \phi \quad (5.11)$$

$$d\theta = \frac{\Omega}{\omega} d\phi, \quad dt = \frac{1}{\omega} d\phi$$

which leads to the following average directional factor:

$$[D_0] = \frac{1}{\phi_p - \phi_{st}} \int_{\phi_{st}}^{\phi_{ex}} D(\phi) d\phi \quad (5.12)$$

Main differences between frequency domain solution of circular milling and regular milling are varying entry ϕ_{st} and exit ϕ_{ex} angles of the tool that determine the limits of integration in circular milling operation. Entry angle ϕ_{st} is assumed to be $\phi_{st} = 0$, and exit angle ϕ_{ex} is assumed to be $\phi_{ex} = \max(\phi_{ex})$ to carry out the integration. Exit angle ϕ_{ex} is taking its maximum value when

the tool is close to center of the circular slot as mentioned in Chapter 3. New immersion dependent average directional milling coefficients are given as follows:

$$\begin{aligned}
 \alpha_{xx} &= \left[-K_r \phi + \frac{1}{2} \left(\frac{H}{H+1} \right) \cos \left(2\phi \left(\frac{H+1}{H} \right) \right) + \frac{1}{2} K_r \left(\frac{H}{H+1} \right) \sin \left(2\phi \left(\frac{H+1}{H} \right) \right) \right] \Bigg|_{\phi_{st}}^{\phi_{ex}} \\
 \alpha_{xy} &= \left[-\phi - \frac{1}{2} \left(\frac{H}{H+1} \right) \sin \left(2\phi \left(\frac{H+1}{H} \right) \right) + \frac{1}{2} K_r \left(\frac{H}{H+1} \right) \cos \left(2\phi \left(\frac{H+1}{H} \right) \right) \right] \Bigg|_{\phi_{st}}^{\phi_{ex}} \\
 \alpha_{yx} &= \left[\phi - \frac{1}{2} \left(\frac{H}{H+1} \right) \sin \left(2\phi \left(\frac{H+1}{H} \right) \right) + \frac{1}{2} K_r \left(\frac{H}{H+1} \right) \cos \left(2\phi \left(\frac{H+1}{H} \right) \right) \right] \Bigg|_{\phi_{st}}^{\phi_{ex}} \\
 \alpha_{yy} &= \left[-K_r \phi - \frac{1}{2} \left(\frac{H}{H+1} \right) \cos \left(2\phi \left(\frac{H+1}{H} \right) \right) - \frac{1}{2} K_r \left(\frac{H}{H+1} \right) \sin \left(2\phi \left(\frac{H+1}{H} \right) \right) \right] \Bigg|_{\phi_{st}}^{\phi_{ex}}
 \end{aligned} \tag{5.13}$$

The resultant dynamic cutting forces are defined by substituting the zero order term of Fourier series $[D_0]$ (Equation (5.12)) into dynamic cutting forces expression in time domain given by Equation (5.7):

$$\{F(t)\} = \frac{1}{2} K_{tc} b [D_0] \{\Delta(t)\} \tag{5.14}$$

where

$$[D_0] = \frac{N}{2\pi} \begin{bmatrix} \alpha_{xx} & \alpha_{xy} \\ \alpha_{yx} & \alpha_{yy} \end{bmatrix}$$

The vibrations $\{\Delta(i\omega)\}$ are written in terms of dynamic cutting forces $\{F(i\omega)\}$ and frequency response function of the machine tool structure $[\Phi(i\omega)]$.

$$\{F(i\omega)\} = \frac{1}{2} K_{tc} b [D_0] \{\Delta(i\omega)\} \tag{5.15}$$

$$\begin{Bmatrix} \Delta x(i\omega) \\ \Delta y(i\omega) \end{Bmatrix} = (1 - e^{-i\omega\tau})[\Phi(i\omega)] \begin{Bmatrix} F_x(i\omega) \\ F_y(i\omega) \end{Bmatrix} \quad (5.16)$$

where

$$\{\Delta(i\omega)\} = \begin{Bmatrix} \Delta x(i\omega) \\ \Delta y(i\omega) \end{Bmatrix} = (1 - e^{-i\omega\tau}) \begin{Bmatrix} x(i\omega) \\ y(i\omega) \end{Bmatrix}$$

$$\begin{Bmatrix} x(i\omega) \\ y(i\omega) \end{Bmatrix} = [\Phi(i\omega)] \begin{Bmatrix} F_x(i\omega) \\ F_y(i\omega) \end{Bmatrix}$$

As circular milling operation is a two dimensional process, frequency response function matrix contains direct $\Phi_{xx}(i\omega)$, $\Phi_{yy}(i\omega)$ and cross $\Phi_{xy}(i\omega)$, $\Phi_{yx}(i\omega)$ frequency response functions in global x and y directions. Two degrees of freedom are considered to be orthogonal to each other, therefore cross frequency response functions $\Phi_{xy}(i\omega)$, $\Phi_{yx}(i\omega)$ are zero:

$$[\Phi(i\omega)] = \begin{bmatrix} \Phi_{xx}(i\omega) & \Phi_{xy}(i\omega) \\ \Phi_{yx}(i\omega) & \Phi_{yy}(i\omega) \end{bmatrix} = \begin{bmatrix} \Phi_{xx}(i\omega) & 0 \\ 0 & \Phi_{yy}(i\omega) \end{bmatrix} \quad (5.17)$$

Dynamic cutting forces in frequency domain at chatter frequency ω_c are obtained by substituting Equation (5.16) into Equation (5.15):

$$\begin{Bmatrix} F_x \\ F_y \end{Bmatrix} e^{i\omega_c t} = \frac{1}{2} K_{tc} b [D_0] (1 - e^{-i\omega_c \tau}) [\Phi(i\omega_c)] \begin{Bmatrix} F_x \\ F_y \end{Bmatrix} e^{i\omega_c t} \quad (5.18)$$

$$\begin{Bmatrix} F_x \\ F_y \end{Bmatrix} e^{i\omega_c t} \left[I - \frac{1}{2} K_{tc} b [D_0] (1 - e^{-i\omega_c \tau}) [\Phi(i\omega_c)] \right] = 0$$

The stability problem turns into an eigenvalue problem which is easier to solve for a given chatter frequency, ω_c , and has a nontrivial solution when the determinant equals to zero [3]:

$$\det[I + \Lambda[\Phi_0(i\omega_c)]] = 0 \quad (5.19)$$

where

$\Lambda = -\frac{N}{4\pi}K_{tc}b(1 - e^{-i\omega_c\tau})$ is the eigenvalue of the characteristic equation of the system.

$[\Phi_0(i\omega_c)] = \begin{bmatrix} \alpha_{xx} & \alpha_{xy} \\ \alpha_{yx} & \alpha_{yy} \end{bmatrix} [\Phi(i\omega_c)]$ is the oriented frequency response function matrix and characteristic equation becomes a second order polynomial:

$$\det \left[\begin{bmatrix} 1 & 0 \\ 0 & 1 \end{bmatrix} + \Lambda \begin{bmatrix} \alpha_{xx} & \alpha_{xy} \\ \alpha_{yx} & \alpha_{yy} \end{bmatrix} \begin{bmatrix} \Phi_{xx}(i\omega_c) & 0 \\ 0 & \Phi_{yy}(i\omega_c) \end{bmatrix} \right] = 0 \quad (5.20)$$

$$h_0\Lambda^2 + h_1\Lambda + 1 = 0$$

where

$$h_0 = \Phi_{xx}(i\omega_c)\Phi_{yy}(i\omega_c)(\alpha_{xx}\alpha_{yy} - \alpha_{xy}\alpha_{yx})$$

$$h_1 = \alpha_{xx}\Phi_{xx}(i\omega_c) + \alpha_{yy}\Phi_{yy}(i\omega_c)$$

$$\Lambda = \frac{-h_1 + \sqrt{h_1^2 - 4h_0}}{2h_0} = \Lambda_R + i\Lambda_{Im}$$

Chatter free critical axial depth of cut b_{lim} is given by:

$$b_{lim} = -\Lambda \frac{4\pi}{NK_{tc}(1 - e^{-i\omega_c\tau})} \quad (5.21)$$

where

$$e^{-i\omega_c\tau} = \cos\omega_c\tau - i\sin\omega_c\tau$$

Critical axial depth of cut b_{lim} has to be a real number, hence imaginary part of Equation (5.21) must be zero:

$$b_{lim} = -\frac{2\pi}{NK_{tc}} \left[\frac{\Lambda_R(1 - \cos\omega_c\tau) + \Lambda_{Im} \sin\omega_c\tau}{(1 - \cos\omega_c\tau)} + i \frac{\Lambda_{Im}(1 - \cos\omega_c\tau) + \Lambda_R \sin\omega_c\tau}{(1 - \cos\omega_c\tau)} \right] \quad (5.22)$$

$$\frac{\Lambda_{Im}(1 - \cos\omega_c\tau) + \Lambda_R \sin\omega_c\tau}{(1 - \cos\omega_c\tau)} = 0 \quad (5.23)$$

The ratio between the real Λ_R and imaginary Λ_{Im} parts of eigenvalue $\kappa = \frac{\Lambda_{Im}}{\Lambda_R} = \frac{\sin\omega_c\tau}{(1 - \cos\omega_c\tau)}$ is substituted in Equation (5.22) and resultant critical axial depth of cut b_{lim} can be expressed as follows:

$$b_{lim} = -\frac{2\pi\Lambda_R}{NK_{tc}} [1 + \kappa^2] \quad (5.24)$$

In order to obtain the stability lobes, spindle speeds n that correspond to critical axial depth of cut b_{lim} must be evaluated by using κ :

$$\kappa = \frac{\sin\omega_c\tau}{(1 - \cos\omega_c\tau)} = \frac{2 \sin \frac{\omega_c\tau}{2} \cos \frac{\omega_c\tau}{2}}{2 \sin^2 \frac{\omega_c\tau}{2}} = \tan\left(\frac{\pi}{2} - \frac{\omega_c\tau}{2}\right) \quad (5.25)$$

$$\text{where } \kappa = \tan\psi = \tan\left(\frac{\pi}{2} - \frac{\omega_c\tau}{2}\right)$$

Phase angle between current and previous cuts becomes:

$$\omega_c\tau = \pi - 2\psi + 2k\pi = \varepsilon + 2k\pi \quad (5.26)$$

where

k , a positive integer number, represents the number of stability lobes and $\varepsilon = \pi - 2\psi$ is the phase shift between the waves on each side of the chip. Spindle speed n can be expressed as follows:

$$n = \frac{60}{N\tau} \quad (5.27)$$

Stability lobes are formed by plotting the chatter free critical axial depth of cut b_{lim} with corresponding spindle speed n on the same graph. Stability curve is forming a boundary between stable and unstable regions. Since the region above the curve represent unstable cutting, chatter free (smooth) surface finish can be generated by choosing cutting conditions below the curve.

5.3.2. Time Finite Element Analysis (TFEA)

Time finite element analysis was established by Bayly et al. [7] for SDOF interrupted cutting operations such as milling to predict the stability and prevent chatter vibrations. Later the method was extended to 2DOF and higher cases by Bayly et al. [8]. The method can also be used for the stability of interrupted metal cutting processes such as circular milling operation. In this subsection, theory behind the extended time finite element analysis is introduced and application to circular milling operation is explained.

A general 2-DOF milling system with an endmill is given in Figure 5.1. The equation of motion of the system is:

$$\begin{aligned} m_x \ddot{x}(t) + c_x \dot{x}(t) + k_x x(t) &= \sum_{j=1}^N g(\phi_j) [-F_{tj} \cos \phi_j - F_{rj} \sin \phi_j] \\ m_y \ddot{y}(t) + c_y \dot{y}(t) + k_y y(t) &= \sum_{j=1}^N g(\phi_j) [F_{tj} \sin \phi_j - F_{rj} \cos \phi_j] \end{aligned} \quad (5.28)$$

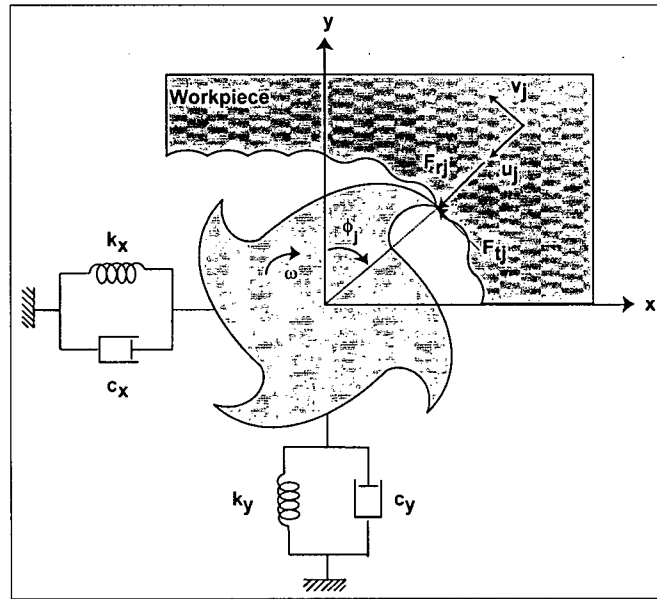


Figure 5.1 : General representation of 2-DOF milling system

In order to obtain resultant equation of motion, tangential $F_{tj} = K_{tc}bh_j$ and radial $F_{rj} = K_{rc}bh_j$ cutting forces acting on tooth j and dynamic chip thickness $h_j = s_t \sin \phi_j + [x(t) - x(t - \tau)] \sin \phi_j + [y(t) - y(t - \tau)] \cos \phi_j$ expressions are substituted in Equation (5.28):

$$[M]\ddot{\vec{x}}(t) + [C]\dot{\vec{x}}(t) + [K]\vec{x}(t) = [K_c(\phi)]b[\vec{x}(t) - \vec{x}(t - \tau)] + b\vec{f}_0(\phi) \quad (5.29)$$

where

$$[M] = \begin{bmatrix} m_x & 0 \\ 0 & m_y \end{bmatrix}, [C] = \begin{bmatrix} c_x & 0 \\ 0 & c_y \end{bmatrix}, [K] = \begin{bmatrix} k_x & 0 \\ 0 & k_y \end{bmatrix}, \vec{x} = \begin{Bmatrix} x(t) \\ y(t) \end{Bmatrix}$$

$$[K_c(\phi)] = \sum_{j=1}^N g(\phi_j) \begin{bmatrix} -K_{tc} \cos \phi_j \sin \phi_j - K_{rc} \sin^2 \phi_j & -K_{tc} \cos^2 \phi_j - K_{rc} \sin \phi_j \cos \phi_j \\ K_{tc} \sin^2 \phi_j - K_{rc} \cos \phi_j \sin \phi_j & K_{tc} \sin \phi_j \cos \phi_j - K_{rc} \cos^2 \phi_j \end{bmatrix}$$

$$\vec{f}_0(\phi) = \sum_{j=1}^N g(\phi_j) \vec{s}_t \begin{bmatrix} -K_{tc} \cos \phi_j \sin \phi_j - K_{rc} \sin^2 \phi_j \\ K_{tc} \sin^2 \phi_j - K_{rc} \cos \phi_j \sin \phi_j \end{bmatrix}$$

Time finite element method subdivides the low immersion milling operation in two parts: cutting (forced or chatter vibration) and not cutting (free vibration). The method divides the time in cut into multiple finite time elements shown in Figure 5.2 and defines x and y displacements approximately at the beginning and end of each element during each pass as a linear combination of polynomial trial functions. Displacement of the tool on q^{th} element during w^{th} pass of the tooth is:

$$\dot{\hat{x}}^w(t) = \sum_{i=1}^4 \dot{\hat{a}}_{qi}^w \cdot \dot{\gamma}_i(t_{local}). \quad (5.30)$$

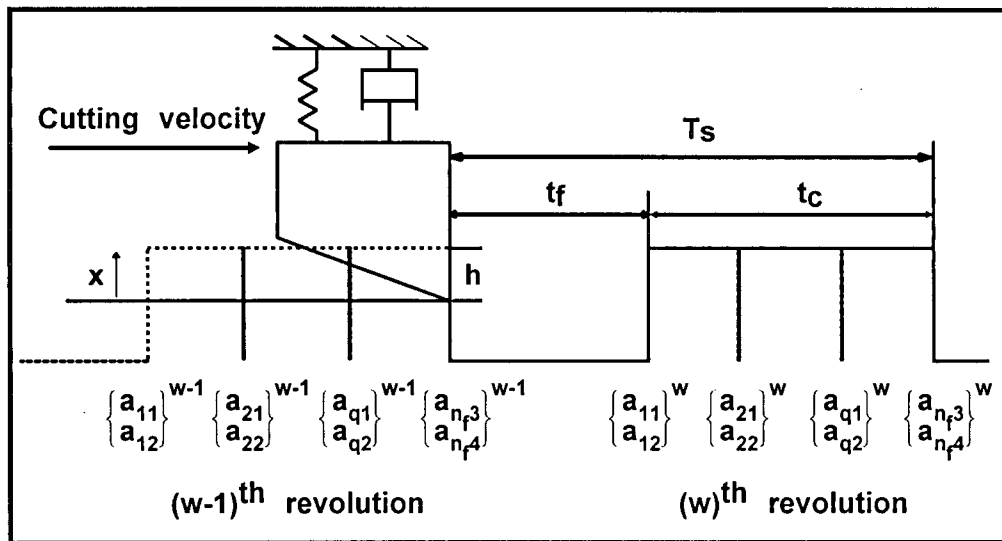


Figure 5.2 : Time finite element method developed for interrupted cutting operations

Velocity and acceleration on q^{th} element during w^{th} pass of the tooth are:

$$\dot{\hat{v}}^w(t) = \dot{\hat{x}}^w(t) = \sum_{i=1}^4 \dot{\hat{a}}_{qi}^w \cdot \dot{\gamma}_i(t_{local}), \quad \ddot{\hat{v}}^w(t) = \ddot{\hat{x}}^w(t) = \sum_{i=1}^4 \ddot{\hat{a}}_{qi}^w \cdot \ddot{\gamma}_i(t_{local}) \quad (5.31)$$

where

$\hat{a}_{q1}^w, \hat{a}_{q2}^w, \hat{a}_{q3}^w, \hat{a}_{q4}^w$ are the coefficients of the polynomials for q^{th} element and t_{local} expresses the local time in q^{th} element during w^{th} pass of the tooth:

$$t_{local}(t) = t - w\tau - \sum_{k=1}^{q-1} t_k \quad (5.32)$$

where $0 \leq t_{local} \leq t_q$, t defines total time, t_k is time length of k^{th} element. If the length of all elements are same, t_k can be given as follows:

$$t_k = \left(\frac{\phi_{ex} - \phi_{st}}{2\pi} \right) \frac{N\tau}{n_f} \quad (5.33)$$

n_f shows the total number of finite elements. Total time passed during cutting t_c is:

$$t_c = \sum_{k=1}^{n_f} t_k \quad (5.34)$$

$\gamma_i(t_{local})$, cubic Hermite polynomials that are selected for their boundary conditions, given in Equation (5.30) are trial functions:

$$\begin{aligned}
\gamma_1(t_{local}) &= 1 - 3\left(\frac{t_{local}}{t_q}\right)^2 + 2\left(\frac{t_{local}}{t_q}\right)^3 \\
\gamma_2(t_{local}) &= t_q \cdot \left\{ \left(\frac{t_{local}}{t_q}\right) - 2\left(\frac{t_{local}}{t_q}\right)^2 + \left(\frac{t_{local}}{t_q}\right)^3 \right\} \\
\gamma_3(t_{local}) &= 3\left(\frac{t_{local}}{t_q}\right)^2 - 2\left(\frac{t_{local}}{t_q}\right)^3 \\
\gamma_4(t_{local}) &= t_q \cdot \left\{ -\left(\frac{t_{local}}{t_q}\right)^2 + \left(\frac{t_{local}}{t_q}\right)^3 \right\}
\end{aligned} \tag{5.35}$$

$$\begin{aligned}
\gamma_1(0) &= 1, \dot{\gamma}_1(0) = 0, \gamma_1(t_q) = 0, \dot{\gamma}_1(t_q) = 0 \\
\gamma_2(0) &= 0, \dot{\gamma}_2(0) = 1, \gamma_2(t_q) = 0, \dot{\gamma}_2(t_q) = 0 \\
\gamma_3(0) &= 0, \dot{\gamma}_3(0) = 0, \gamma_3(t_q) = 1, \dot{\gamma}_3(t_q) = 0 \\
\gamma_4(0) &= 0, \dot{\gamma}_4(0) = 0, \gamma_4(t_q) = 0, \dot{\gamma}_4(t_q) = 1
\end{aligned} \tag{5.36}$$

Because of the boundary conditions stated in Equation (5.36), the displacement $\dot{x}(t)$ and velocity $\dot{v}(t)$ at the beginning ($t_{local} = 0$) and end ($t_{local} = t_q$) of q^{th} element during w^{th} pass of the tooth are equal to one of the coefficients $\ddot{a}_{q1}, \ddot{a}_{q2}, \ddot{a}_{q3}, \ddot{a}_{q4}$ of the polynomials:

Displacement $\dot{x}(t)$ and velocity $\dot{v}(t)$ on q^{th} element at initial point ($t_{local} = 0$):

$$\dot{x}(t_{bq}^w) = \ddot{a}_{q1}^w \quad \dot{v}(t_{bq}^w) = \ddot{a}_{q2}^w$$

Displacement $\dot{x}(t)$ and velocity $\dot{v}(t)$ on q^{th} element at final point ($t_{local} = t_q$):

$$\dot{x}(t_{eq}^w) = \ddot{a}_{q3}^w \quad \dot{v}(t_{eq}^w) = \ddot{a}_{q4}^w \quad \text{where } t_{bq}^w = w\tau + \sum_{k=1}^{q-1} t_k, \quad t_{eq}^w = w\tau + \sum_{k=1}^q t_k$$

Time delay displacement of q^{th} element $\dot{x}(t-\tau)$ is obtained from the approximately defined displacement of q^{th} element $\dot{x}(t)$ given by Equation (5.30):

$$\dot{x}(t-\tau) = \sum_{i=1}^4 \ddot{a}_{qi}^{w-1} \cdot \gamma_i(t_{local}) \tag{5.37}$$

Since the displacement on q^{th} element $\dot{\hat{x}}(t)$ is determined approximately, a non-zero error is formed when the displacement expression (Equation (5.30)) is substituted in equation of motion of the 2DOF milling system (Equation (5.29)). A set of test functions, $\eta_p(t)$ $p = 1, 2$ [16], is used for weighting the error. Later weighted error is set to zero by taking the integral of the equation of motion. Two vector equations are written for each element. $\eta_1(t) = 1$ is chosen in order to measure average error and $\eta_2(t) = t_{local}/t_q - 1/2$ is selected for linearly increasing error.

$$\int_0^{t_q} \left\{ [M] \cdot \left(\sum_{i=1}^4 \dot{\hat{a}}_{qi}^w \cdot \ddot{\gamma}_i \cdot \eta_p \right) + [C] \cdot \left(\sum_{i=1}^4 \dot{\hat{a}}_{qi}^w \cdot \dot{\gamma}_i \cdot \eta_p \right) + [K] \cdot \left(\sum_{i=1}^4 \dot{\hat{a}}_{qi}^w \cdot \gamma_i \cdot \eta_p \right) \right\} dt_{local} - \int_0^{t_q} b \cdot \left\{ \vec{f}_0(\phi) \cdot \eta_p + [K_c(\phi)] \left(\sum_{i=1}^4 \dot{\hat{a}}_{qi}^w \cdot \gamma_i \cdot \eta_p \right) - [K_c(\phi)] \left(\sum_{i=1}^4 \dot{\hat{a}}_{qi}^{w-1} \cdot \gamma_i \cdot \eta_p \right) \right\} dt_{local} = 0 \quad (5.38)$$

Two algebraic equations for element q are obtained in matrix form by calculating the definite integral given by Equation (5.38):

$$\begin{bmatrix} N_{11} & N_{12} & N_{13} & N_{14} \\ N_{21} & N_{22} & N_{23} & N_{24} \end{bmatrix} \begin{Bmatrix} \dot{\hat{a}}_{q1} \\ \dot{\hat{a}}_{q2} \\ \dot{\hat{a}}_{q3} \\ \dot{\hat{a}}_{q4} \end{Bmatrix}^w = \begin{Bmatrix} \vec{C}_1 \\ \vec{C}_2 \end{Bmatrix} + \begin{bmatrix} P_{11} & P_{12} & P_{13} & P_{14} \\ P_{21} & P_{22} & P_{23} & P_{24} \end{bmatrix} \begin{Bmatrix} \dot{\hat{a}}_{q1} \\ \dot{\hat{a}}_{q2} \\ \dot{\hat{a}}_{q3} \\ \dot{\hat{a}}_{q4} \end{Bmatrix}^{w-1} \quad (5.39)$$

where

$$N_{pi} = \int_0^{t_q} \{ [M] \ddot{\gamma}_i + [C] \dot{\gamma}_i + ([K] - b[K_c(\phi)]) \gamma_i \} \eta_p dt_{local} \quad (2 \times 2)$$

$$\vec{C}_p = \int_0^{t_q} b \vec{f}_0(\phi) \eta_p dt_{local} \quad (2 \times 1)$$

$$P_{pi} = - \int_0^{t_q} b [K_c(\phi)] \gamma_i \eta_p dt_{local} \quad (2 \times 2)$$

As $[K_c(\phi)]$ and $\vec{f}_0(\phi)$ are dependent on instantaneous immersion angle ϕ , for evaluating Equation (5.39) immersion angle has to be expressed in terms of local time in q^{th} element t_{local} :

$$\phi(t_{local}) = 2\pi \left(\frac{t_{local} + \sum_{k=1}^{q-1} t_k}{(60/n)} \right) = \omega \left(t_{local} + \sum_{k=1}^{q-1} t_k \right) \quad (5.40)$$

The displacement and velocity vectors at the end of q^{th} element ($t_{local} = t_q$) are equal to the displacement and velocity vectors at the beginning of $(q+1)^{th}$ element ($t_{local} = 0$) during cutting:

$$\begin{Bmatrix} \dot{\vec{a}}_{q3} \\ \dot{\vec{a}}_{q4} \end{Bmatrix}^w = \begin{Bmatrix} \dot{\vec{a}}_{(q+1)1} \\ \dot{\vec{a}}_{(q+1)2} \end{Bmatrix}^w \quad (5.41)$$

When the tool is out of the cut (free vibration), displacement and velocity relations in one direction between finite elements are given as follows:

$$\begin{Bmatrix} \dot{\vec{a}}_{11} \\ \dot{\vec{a}}_{12} \end{Bmatrix}^w = [e^{[F]t_f}] \begin{Bmatrix} \dot{\vec{a}}_{n3} \\ \dot{\vec{a}}_{n4} \end{Bmatrix}^{w-1} \quad (5.42)$$

where

$$[F] = - \begin{bmatrix} 0 & [M] \\ [I] & 0 \end{bmatrix}^{-1} \begin{bmatrix} [K] & [C] \\ 0 & -[I] \end{bmatrix}$$

$t_f = \tau - t_c$ is time passed during free vibration (not cutting).

Dynamics of milling operation is defined in terms of present and previous revolutions by substituting the boundary relations between finite elements given by Equation (5.41) and Equation (5.42) into Equation (5.39) in order to obtain the coefficients $\dot{\bar{a}}_{q1}, \dot{\bar{a}}_{q2}, \dot{\bar{a}}_{q3}, \dot{\bar{a}}_{q4}$:

$$\begin{bmatrix} I & 0 & 0 & \dots & 0 & 0 \\ N_1 & N_2 & 0 & \dots & 0 & 0 \\ 0 & N_1 & N_2 & \dots & 0 & 0 \\ 0 & 0 & 0 & \dots & 0 & 0 \\ 0 & 0 & 0 & \dots & N_2 & 0 \\ 0 & 0 & 0 & \dots & N_1 & N_2 \end{bmatrix} \begin{bmatrix} \dot{\bar{a}}_{11} \\ \dot{\bar{a}}_{12} \\ \dot{\bar{a}}_{21} \\ \dot{\bar{a}}_{22} \\ \dots \\ \dot{\bar{a}}_{n_f1} \\ \dot{\bar{a}}_{n_f2} \\ \dot{\bar{a}}_{n_f3} \\ \dot{\bar{a}}_{n_f4} \end{bmatrix}^w = \begin{bmatrix} 0 & 0 & 0 & \dots & 0 & e^{[F]t_f} \\ P_1 & P_2 & 0 & \dots & 0 & 0 \\ 0 & P_1 & P_2 & \dots & 0 & 0 \\ 0 & 0 & 0 & \dots & 0 & 0 \\ 0 & 0 & 0 & \dots & P_2 & 0 \\ 0 & 0 & 0 & \dots & P_1 & P_2 \end{bmatrix} \begin{bmatrix} \dot{\bar{a}}_{11} \\ \dot{\bar{a}}_{12} \\ \dot{\bar{a}}_{21} \\ \dot{\bar{a}}_{22} \\ \dots \\ \dot{\bar{a}}_{n_f1} \\ \dot{\bar{a}}_{n_f2} \\ \dot{\bar{a}}_{n_f3} \\ \dot{\bar{a}}_{n_f4} \end{bmatrix}^{w-1} + \begin{bmatrix} \dot{\bar{C}}_{11} \\ \dot{\bar{C}}_{12} \\ \dot{\bar{C}}_{21} \\ \dot{\bar{C}}_{22} \\ \dots \\ \dot{\bar{C}}_{n_f1} \\ \dot{\bar{C}}_{n_f2} \\ \dot{\bar{C}}_{n_f3} \\ \dot{\bar{C}}_{n_f4} \end{bmatrix} \quad (5.43)$$

where

$$\begin{aligned} N_1 &= \begin{bmatrix} N_{11} & N_{12} \\ N_{21} & N_{22} \end{bmatrix}_{(4 \times 4)} & N_2 &= \begin{bmatrix} N_{13} & N_{14} \\ N_{23} & N_{24} \end{bmatrix}_{(4 \times 4)} \\ P_1 &= \begin{bmatrix} P_{11} & P_{12} \\ P_{21} & P_{22} \end{bmatrix}_{(4 \times 4)} & P_2 &= \begin{bmatrix} P_{13} & P_{14} \\ P_{23} & P_{24} \end{bmatrix}_{(4 \times 4)} \end{aligned} \quad (5.44)$$

The dimension of global $[N]$ and $[P]$ matrices in Equation (5.43) is $(4n_f + 4) \times (4n_f + 4)$ and the dimension of global $[C]$ matrix is $(4n_f + 4) \times 1$. Linear discrete dynamical system given by Equation (5.43) can be described as:

$$\dot{\bar{a}}^w = [Q]\dot{\bar{a}}^{w-1} + [\dot{S}] \quad (5.45)$$

where

$$[N]\dot{\vec{a}}^w = [P]\dot{\vec{a}}^{w-1} + [\vec{C}]$$

$$[Q] = [N]^{-1}[P]$$

$$[\vec{S}] = [N]^{-1}[\vec{C}]$$

By verifying magnitudes of eigenvalues of $[Q]$ matrix, stability of 2DOF milling system is determined. If one of the magnitudes is greater than 1, the system is unstable.

In order to investigate the stability of circular milling operations, the application of the time finite element method has to be explained. $[K_c]$ and \vec{f}_0 in Equation (5.29) are different from regular 2-DOF milling operation because of the planetary motion of the tool. $[K_c]$ and \vec{f}_0 are dependent on not only instantaneous immersion angle ϕ but also angular position of the tool θ :

$$[K_c(\phi)] = \sum_{j=1}^N \frac{1}{2} g(\phi_j) K_{tc} \begin{bmatrix} -K_r - \sin 2E + K_r \cos 2E & -1 - K_r \sin 2E - \cos 2E \\ 1 - \cos 2E - K_r \sin 2E & -K_r - K_r \cos 2E + \sin 2E \end{bmatrix} \quad (5.46)$$

$$\vec{f}_0(\phi) = \sum_{j=1}^N \frac{1}{2} g(\phi_j) s_t K_{tc} \begin{bmatrix} -\sin(\phi_j) \cos E - K_r \sin(\phi_j) \sin E \\ \sin(\phi_j) \sin E - K_r \sin(\phi_j) \cos E \end{bmatrix}$$

In order to eliminate one of the variables, the relation between instantaneous immersion angle ϕ and angular position of the tool θ given by Equation (5.11) ($\theta = \frac{\phi}{H}$, $E = \phi_j + \frac{\phi}{H}$) is substituted in Equation (5.46).

Exit angle ϕ_{ex} (immersion) is assumed to be constant during one tooth passing period and is calculated as mentioned in Chapter 3 for the starting condition of each tooth passing period ($\theta = \Omega \frac{2\pi r}{\omega}$, $r = 0, 1, 2, \dots \rightarrow$ number of tooth passing periods) while variation of exit angle ϕ_{ex} is calculated by time finite element method.

The planetary motion of the tool is modeled in time finite element method by summing up the successive rotations of the tool around itself to form the circular toolpath around the workpiece. Global $[N]$, $[P]$ and $[C]$ matrices in Equation (5.43) are different for each tooth passing period since $[K_c(\phi, \theta)]$ and $\vec{f}_0(\phi, \theta)$ in Equation (5.46) are changing as the angular position of the tool θ alters.

Although the immersion as well as time in cut t_c varies during circular milling operation, the number of finite elements n_f is kept constant for each tooth passing period by changing the length of elements t_k from one tooth passing period to another to make the size of the global $[N]$, $[P]$, $[C]$ and \dot{a}_{qi} matrices given by Equation (5.43) equal. Time in cut t_c is divided in such a way that all the finite elements have the same time length during one tooth passing period.

The stability of the circular milling system is obtained by verifying magnitudes of the dynamic displacements at the end of one tooth passing period of the tool around the workpiece. If the dynamic displacements increase exponentially, the system behaves unstable, otherwise it is stable. The periodicity coming from successive revolutions of the tool around the workpiece is ignored during the simulations.

5.4. Simulations and Experimental Results

In the previous sections, dynamics of circular milling operation have been introduced and two analytical approaches have been explained in detail. In order to verify the chatter stability models for circular milling, experiments were held for a range of axial depth of cut and spindle speed values, which are given in the Table 5.3. An end mill having $R_c = 10$ [mm] radius and $N = 4$ teeth was used. Al 7075T6 was used as the workpiece. The tangential and radial cutting force coefficients obtained experimentally by using mechanistic approach were $K_{tc} = 796.077$ [N/mm²] and $K_{rc} = 168.829$ [N/mm²]. The step over feed $c = 5.7738$ [mm], the feed rate per tooth $s_t = 0.1$ [mm/rev/tooth], the width of the slot $R_s = 25$ [mm], the maximum immersion angle $\phi_{max} = 65^\circ$ and the ratio between speeds $H = 235.6$ were determined as cutting conditions for the experiments. Chatter detection is made based on the ratio of dynamic over static chip thickness as well as the frequency content of both cutting force and tool vibration. The modal parameters in x and y directions given by the Table 5.1 and Table 5.2 are used in both the frequency domain and time finite element simulations:

Table 5.1 : Modal parameters in x direction

Mode Number	Natural Frequency ω_n [Hz]	Damping Ratio ξ	Stiffness k [N/mm]
1	486	0.0463	9.41×10^4
2	617	0.0138	38.06×10^4
3	714	0.0175	9.51×10^4
4	1007	0.0556	2.37×10^4
5	1380	0.0137	155.77×10^4
6	1874	0.0200	43.4×10^4
7	2270	0.0233	22.57×10^4
8	2770	0.0184	23.03×10^4
9	3010	0.0183	32.32×10^4
10	4059	0.0083	23.65×10^4

Table 5.2 : Modal parameters in y direction

Mode Number	Natural Frequency ω_n [Hz]	Damping Ratio ξ	Stiffness k [N/mm]
1	759	0.0315	4.43×10^4
2	980	0.0444	5.97×10^4
3	1695	0.0177	82.6×10^4
4	1909	0.0079	272.57×10^4
5	2045	0.0086	219.89×10^4
6	2395	0.0192	32.55×10^4
7	2770	0.0181	32.69×10^4
8	3010	0.0191	37.94×10^4
9	4045	0.0136	21.13×10^4

Table 5.3 : Axial depth of cut (b) and spindle speed (n) values for cutting tests and simulations

Test no	Axial depth of cut b [mm]	Spindle speed n [rpm]	Stability (Experiment)	Stability (TFEA)	Stability (Frequency)
1	6	1511	S	S	S
2	6	1992	S	S	S
3	11	3000	S	S	US
4	11	3501	US	S	S
5	11	3750	S	S	S
6	11	4211	US	US	US
7	8	4188	S	S	S
8	11	4600	US	US	S
9	11	5201	US	S	S
10	8	5185	S	S	S
11	11	5850	S	S	CS
12	11	6598	US	US	US
13	8	6594	S	S	CS
14	11	7205	US	US	US
15	11	7515	US	US	CS
16	8	7506	S	S	S
17	11	8024	US	S	S
18	8	8000	S	S	S

S, US and CS are used for stable, unstable and critically stable cuts respectively in Table 5.3. Common cutting parameters are given in Table 5.4:

Table 5.4 : Common cutting conditions

Workpiece=Al 7075T6
N=4 teeth (endmill)
$R_c=10$ [mm]
$K_{tc}=796.077$ [N/mm ²]
$K_{rc}=168.829$ [N/mm ²]
$R_s=25$ [mm]
$c=5.7738$ [mm]
$s_t=0.1$ [mm/rev/tooth]
$\phi_{max} = 65^\circ$
H=235.6

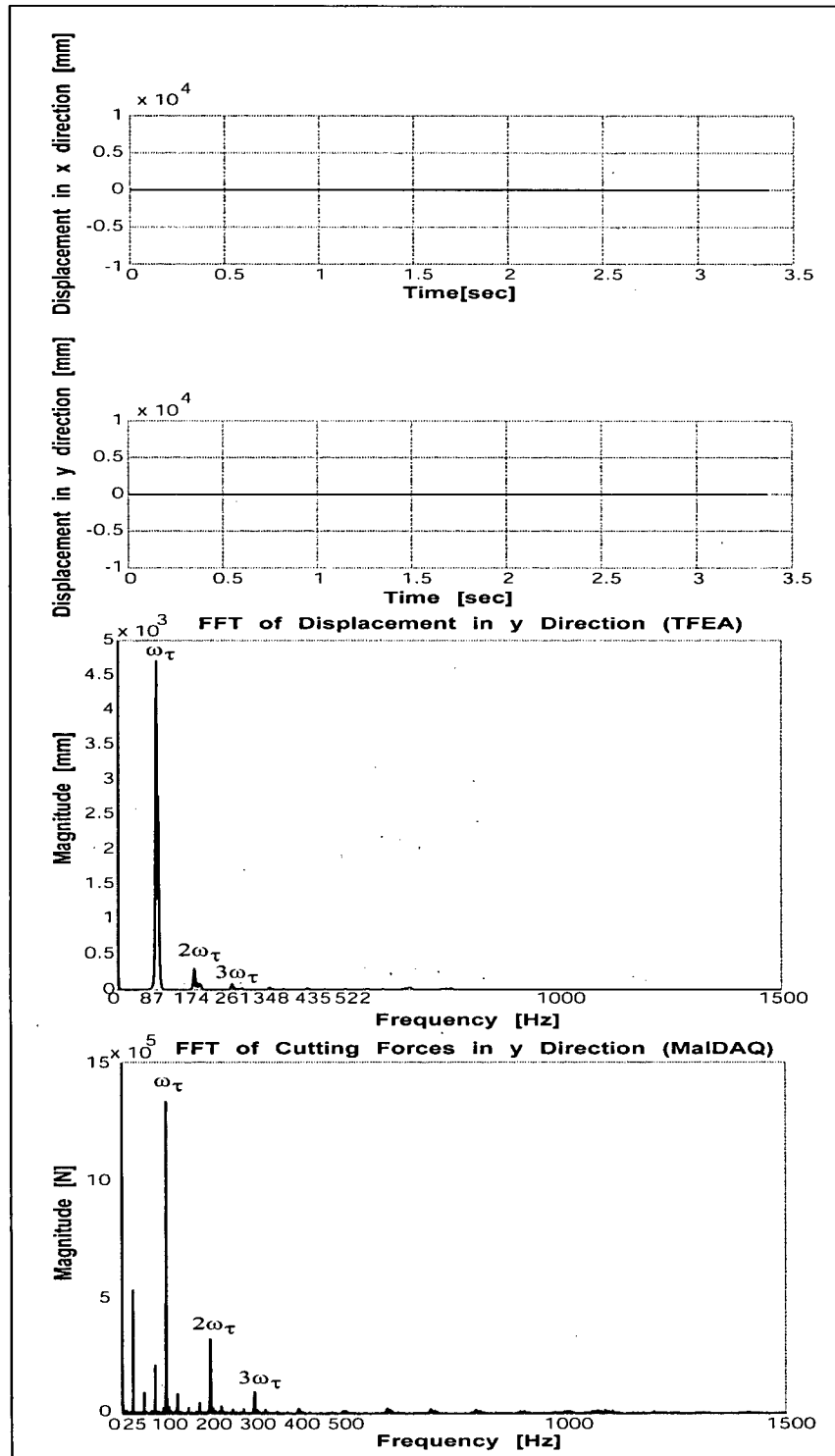


Figure 5.3 : Simulated displacements for a stable circular milling operation cutting conditions ($n=1500$ [rpm] and $b=6$ [mm], See Table 5.3)

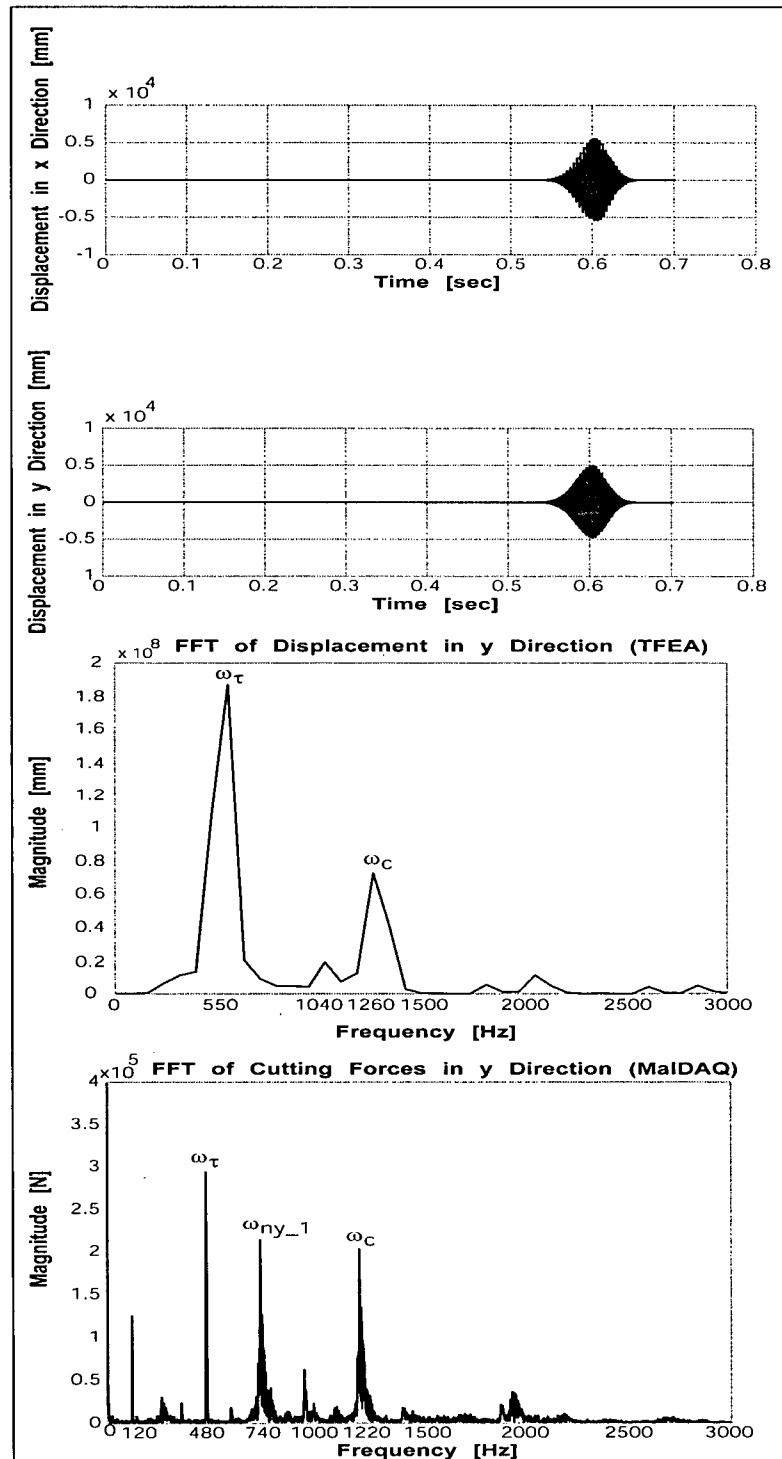


Figure 5.4 : Simulated displacements for a stable circular milling operation cutting conditions ($n=7200$ [rpm] and $b=11$ [mm], See Table 5.3)

In order to simplify the solution and shorten the simulation time & required memory for time finite element analysis, only one mode is taken into account from each direction. The 4th mode of x direction and the 1st mode of y direction are considered as they are the most flexible modes in these directions. The time finite element simulation results for stable (test 1) and unstable (test 14) cutting and FFT's are given as an example in Figure 5.3 and Figure 5.4.

The chatter frequency for the unstable cutting condition obtained from time finite element analysis is $\omega_c = 1260$ [Hz] as shown in Figure 5.4. The chatter frequency in the experimental result for the same cutting condition is $\omega_c = 1220$ [Hz]. Since the time length of the elements are different for each tooth passing period, the data are resampled in order to take FFT. The difference between the chatter frequencies is coming from the resampling of the data obtained from the displacement simulation.

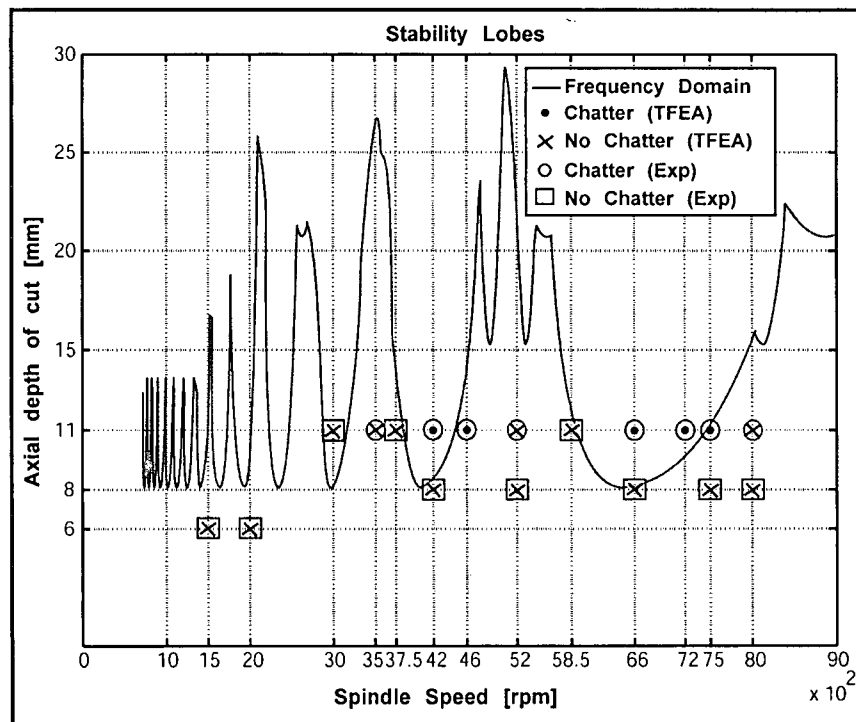


Figure 5.5 : Comparison of experimental and theoretical results

The experimental and simulation results are compared in Figure 5.5. The continuous curve, the stability curve is predicted in frequency domain by averaging time varying directional factors.

Although the directional factors vary both in tooth and circular feed periods, their average leads to linear frequency domain solution which is computationally efficient and practical. However the frequency domain solution does not lead to accurate prediction of stability pockets and can be considered only for speed independent or low axial depth of cut region around 8 [mm]. The time finite element simulation considers the time varying directional factors but does not show any improvement over frequency domain solution either. Although it is computationally several orders of magnitude more costly.

Chapter 6

Conclusion

6.1. Conclusion

Mechanics and chatter stability of circular milling operations are studied in the thesis.

First, the mechanics of circular milling is developed by modelling the kinematics of cutter motion and intersection with the workpiece. The dynamically changing cutter engagement conditions are mathematically modelled as a function of cutter radius, orbital radius of the tool path, spindle speed, step-over feed of the path, and feed rate. Since the immersions, the cutter engagement conditions, change continuously during circular milling, chip thickness and cutting forces vary with cutter position and time. The operation is simulated at discrete time intervals and the immersions, chip thickness and the cutting forces are predicted for chatter vibration free cutting conditions. The chip load and the static cutting forces are calculated and compared well against experimental results.

The circular milling has double periodicity with two time delays and time varying directional factors. The stability problem belongs to delayed differential equations with time varying parameters. First, the stability of milling with single delays is investigated by investigating the applicability of direct stability method proposed by Olgac and Sipahi [31] for time invariant, delayed differential equations. In direct method, the equation of motion for the milling system is defined in state space, and the time delay term is replaced by a bilinear expression [29] which is valid when the system is critically stable. Routh-Hurwitz array is formed by using the coefficients of the characteristic equation, which leads to the stability check of the system for each trial cutting speed and depth of cut. It is shown that Direct Method leads to the same solution with Frequency Domain stability law proposed by Altintas and Budak [11, 12], but with higher computational cost. Direct method still uses the frequency domain mathematical model of the process where time varying, periodic directional factors are assumed to be constant by averaging them. It is not possible to extend the direct method to the case where parameters are time variant, which is the

fundamental issue in circular milling. Hence, the stability of the circular milling is studied in frequency domain by extending the method proposed by Altintas and Budak [11, 12], as well as time domain method presented by Bayly et al. [7, 8].

The dynamics of the circular milling is modelled in time domain by considering the structural vibrations in two orthogonal directions. The dynamic model consists of two coupled differential equations with time varying parameters which are periodic at the tooth passing frequency as well as circular path frequency. Typically, the circular path frequency is at least an order of magnitude less than the tooth passing frequency. The cutting forces which excite the structure have a delay term which is equal to the tooth period. The stability is studied in frequency domain by linearizing the process as follows. The time variation of directional factors are opened to Fourier Series by considering the double periodicity. The circular path frequency is assumed to be a known integer ratio of the tooth passing frequency. By taking the average of the directional factors at tooth and circular path periods, the equation of motion became time invariant and linear. Also, the time variation of the immersion is neglected by considering the worst immersion which becomes highest at the center of the path. The stability of the process is solved by extending the chatter law presented by Budak and Altintas [11, 12]. The stability lobes obtained from the frequency domain solution did not lead to perfect agreement with experimental results due to approximations made to linearize the system dynamics.

In order to include the time varying dynamics of the process, the stability is solved numerically in time domain. The time finite element analysis presented by Bayly et al. [7, 8] is applied to circular milling. The time in cut is divided into multiple finite elements, and displacements on each element are defined in terms of shape functions and boundary conditions. The system becomes a linear discrete map and the stability is tested by checking the magnitudes of the eigenvalues. Dynamic displacements are simulated and used to determine the stability. Only the most flexible modes in x and y directions are chosen in order to reduce the running time and complexity of the MATLAB program. The displacement simulations are compared against the experimental results and they are not in good consistency because of the assumptions made to simplify the solution. As the time finite element method is a linear analysis, the method neglects the saturation of the process such as tool jumping out of cut. By taking the difference between the displacements

of successive passes and checking whether the tool is in cut, saturation of the process may be implemented to time finite element analysis. After determining the elements where the tool jumps out of cut, free vibration equations are substituted into the equation of motion matrix of circular milling and the simulation is repeated for new conditions.

Both frequency domain solution and time finite element method give reasonable results at low axial depth of cut b values but time finite element method is more time inefficient. Time finite element leads to exact numerical solution but the matrix sizes become unmanageable if more than one structural mode is considered in each direction. The prediction may improve all active modes are considered. However even a simulation of a single mode in each direction takes about twenty five minutes on Pentium IV CPU with 1.50 GHz clock frequency. Hence the required computational cost and matrix sizes do not make time finite element approach feasible in stability lobes. Therefore the circular milling dynamics can be analyzed by the proposed frequency domain solution or computationally efficient, more accurate and new stability laws must be studied.

6.2. Future Research Directions

The mechanics of circular milling requires further research by considering the helical plunge motion of the cutter, which makes the process three dimensional. Only a two dimensional case is studied in this thesis. The helical-circular milling is used as an alternative to boring and straight plunge milling operations.

The chatter stability of the circular milling requires further investigation where the double periodicity and time varying directional factors can be more accurately considered. The study belongs to solution of delayed differential equations with time varying parameters, which is still an unsolved problem in the literature. Instead of linearizing the process, time domain simulation of the circular milling may need to be developed to verify the feasibility of various, approximate analytical solutions.

Bibliography

- [1] Airey, J., Oxford, C. J., 1921, "On the Art of Milling", Transactions of ASME, Vol. 43, pp. 549.
- [2] Altintas, Y., Spence, A., "End Milling Force Algorithms For Cad Systems", Annals of CIRP, Vol. 50(1), pp. 169-175.
- [3] Altintas, Y., 2000, "Manufacturing Automation - Metal Cutting Mechanics, Machine Tool Vibrations, and CNC Design", Cambridge University Press.
- [4] Altintas, Y., 2001, "Analytical Prediction of Three Dimensional Chatter Stability in Milling", Japan Society of Mechanical Engineers, International Journal Series C: Mechanical Systems, Machine Elements and Manufacturing, Vol. 44(3), pp. 717-723.
- [5] Altintas, Y., Weck, M., 2004, "Chatter Stability of Metal Cutting and Grinding", CIRP Annals, Vol. 53/2, pp. 619-642.
- [6] Armarego, E. J. A., Epp, C. J., 1970, "An Investigation of Zero Helix Peripheral Up-Milling", International Journal of Machine Tool Design and Research, Vol. 10, pp. 273-291.
- [7] Bayly, P. V., Halley, J. E., Mann, B. P., Davies, M. A., "Stability of Interrupted Cutting by Temporal Finite Element Analysis", Transactions of the ASME, Vol. 125, pp. 220-225.
- [8] Bayly, P. V., Schmitz, T. L., Gabor, S., Mann, B. P., Peters, D. A., Insperger, T., "Effects of Radial Immersion and Cutting Direction on Chatter Instability in End-Milling", Proceedings of the International Mechanical Engineering Conference and Exposition (IMECE 2002), New Orleans, LA.
- [9] Boston, O. W., Kraus, C. E., 1932, "Elements of Milling", Transactions of ASME, Vol. 54, pp. 74-104.

- [10] Boston, O. W., Kraus, C. E., 1932, "Elements of Milling-Part II", Transactions of ASME, Vol. 56, pp. 355-371.
- [11] Budak, E., 1994, "Mechanics and Dynamics of Milling Thin Walled Structures", Ph.D. Thesis, University of British Columbia.
- [12] Budak, E., Altintas, Y., 1995, "Analytical Prediction of Stability Lobes in Milling", CIRP Annals, Vol. 44, No.1, pp. 357-362.
- [13] Budak, E., Altintas, Y., Armarego E. J. A., 1996, "Prediction of Milling Force Coefficients from Orthogonal Cutting Data", Transactions of ASME, Vol. 118, pp. 216-224.
- [14] Campomanes, M. L., "Dynamics of Milling Flexible Structures", Master's Thesis, University of British Columbia.
- [15] Faassen, R. P. H., Van de Wouw, N., Oosterling, J. A. J., Nijmeijer, H., 2003, "Prediction of Regenerative Chatter by Modelling and Analysis of High Speed Milling", Int. J. Machine Tools and Manufac.
- [16] Hou, L. J., Peters, D. A., 1994, "Application of Triangular Space-time Finite Elements to Problems of Wave Propagation", Journal of Sound and Vibration, Vol. 173, No. 5, pp. 611-632.
- [17] Kline, W. A., DeVor, R. E., Zdeblick, W. J., 1980, "A Mechanistic Model for the Force System in End Milling with Application to Machining Airframe Structures", In North American Manufacturing Research Conference Proceedings Society of Manufacturing Engineers, Vol. 18, pp. 297, Dearborn, MI.
- [18] Koenigsberger, F., Tlustý, J., 1967, "Machine Tool Structures-Vol I: Stability Against Chatter", Pergamon Press.
- [19] Kolmanovskii, V. B., Niculescu, S., "On the Liapunov-Karasovskii Functionals for Stability Analysis of Linear Delay Systems", Int. J. Control, 72(4), 374-384.

- [20] Kuo, C. B., 1987, "Automatic Control Systems", Prentice-Hall.
- [21] Lee, P., 1995, "Mechanics and Dynamics of Ball End Milling", Master's Thesis, University of British Columbia.
- [22] Martellotti, M. E., 1941, "An Analysis of the Milling Process", Transactions of ASME, pp. 677-700.
- [23] Martellotti, M. E., 1945, "An Analysis of the Milling Process Part II: Down Milling", Transactions of ASME, Vol. 67, pp. 233-251
- [24] Merritt, H. E., 1965, "Theory of Self-Excited Machine Tool Chatter", ASME Journal of Engineering for Industry, Vol. 87, pp. 447-454.
- [25] Minis, I., Yanushevsky, T., 1993, "A New Theoretical Approach for the Prediction of Machine Tool Chatter in Milling", ASME Journal of Engineering for Industry, Vol. 115, pp. 1-8.
- [26] Montgomery, D., Altintas, Y., 1991, "Mechanism of Cutting Force and Surface Generation in Dynamic Milling", Transactions of ASME Journal of Engineering for Industry, Vol. 113, pp. 160-168.
- [27] Opitz, H., 1969, "Investigation and Calculation of the Chatter Behavior of: Lathes and Milling Machines", Annals of CIRP, Vol. 18, pp. 335-342.
- [28] Parsons, F., 1923, "Power Required for Cutting Metal", Transactions of ASME, Vol. 49, pp. 193-227.
- [29] Rekasius, Z. V., 1980, "A Stability Test for Systems with Delays", in Proc. Joint Automatic Control Conference, Paper No. TP9-A.
- [30] Sawin, N. N., "Theory of Milling Cutters", Mechanical Engineering, Vol. 48, pp. 1203-1209.

- [31] Sipahi, R., 2000, "A Unique Treatment of Time Delay System Stability: The Direct Method", Master's Thesis, University of Connecticut.
- [32] Sutherland, J. W., DeVor, R. E., 1986, "An Improved Method for Cutting Force and Surface Prediction in Flexible End Milling System", Transactions of ASME Journal of Engineering for Industry, Vol. 108, pp. 269-279.
- [33] Tlustý, J., Poláček, M., 1957, "Beispiele der Behandlung der selbsterregten Schwingung der Werkzeugmaschinen", FoKoMa, Hanser Verlag, München.
- [34] Tlustý, J., 1965, "A Method of Analysis of Machine Tool Stability", Proceeding MTDR, pp. 5-14.
- [35] Tlustý, J., McNeil, P., 1970, "Dynamics of Cutting Forces in End Milling", Annals of the CIRP, Vol. 24, pp. 21-25.
- [36] Tlustý, J., Ismail, F., 1981, "Basic Nonlinearity in Machining Chatter", Annals of the CIRP, Vol. 30, pp. 21-25.
- [37] Tlustý, J., "Personal Communications, September 1999-May 2000", Machine Tool Research Center, University of Florida, Gainesville.
- [38] Tlustý, J., 2000, "Manufacturing Processes and Equipment", Prentice Hall.
- [39] Tobias, S. A., 1965, "Machine Tool Vibration", Blackie and Sons Ltd.
- [40] Tobias, S. A., Fiswick, W., 1958, "Theory of Regenerative Machine Tool Chatter", Engineering, London, Vol. 258.
- [41] Weck, M., Staimer, D., 2002, "Parallel Kinematic Machine Tools - Current State and Future Potentials", CIRP Annals, Vol. 2, pp. 671-683.